



Tectonic Geomorphology studies in South
Australia :
Whyalla's Scarps and Billa Kalina Basin



Report of Second Year of Prédctorat
Ecole Normale Supérieure de Paris
March 2006- August 2006

Contents

Abstract	3
Acknowledgements	4
Introduction	5
1 Numerical Modelling of geomorphological processes	6
1.1 Modelled Processes and equations	6
1.1.1 Short-Range Transport	6
1.1.2 Long-Range Transport	7
1.2 Implementation	8
1.2.1 Background	8
1.2.2 Description of a loop	8
1.2.3 Why IDL ?	10
2 Geomorphologic response of a faulting event	12
2.1 Area of study : Whyalla's scarps	12
2.1.1 Murninnie scarp	14
2.1.2 Randell scarp	14
2.1.3 Age of the Faulting	15
2.2 Field Methods and collected datas	16
2.2.1 High resolution GPS	16
2.2.2 Profiles of the scarps	16
2.3 Modelling the diffusive response faulting events	16
2.3.1 Murninnie scarp	17
2.3.2 Randell scarp	17
2.4 Interpretations / Conclusion	18
3 Landscape Evolution in Billa Kalina Area	19
3.1 The Billa Kalina Basin	22
3.1.1 Stratigraphy	22
3.1.2 Sedimentologic and geomorphic features	25
3.1.3 Interpretations	26
3.2 Adjacents Basins	27
3.2.1 Lake Torrens	28
3.2.2 Lake Eyre	29
3.2.3 Interpretations and conclusions	29
3.3 Tomography and edge-driven convection	30
Conclusion	32
References	33
A Code	36

Abstract

Several ways to study the geomorphology of an area are presented in this report. A numerical model which includes erosion/deposition by channelled flow and diffusion was built in IDL 'Interactive Data Language'. This model was applied in the Eyre Peninsula, in South Australia where there is young scarps. This use of modelling allows us to determine the best values of diffusive coefficient for each fault scarp.

The second part of this study was about Lake Eyre region, one of the biggest internal drainage basins in the world. A precise study of Billa Kalina paleolake and its area permits to determine the landscape evolution of this area. It seems that a significant subsidence occurred in Lake Eyre area since the Late Miocene / Early Pliocene and the hypothesis of influence of downwelling flow in the mantle is expressed.

Résumé

Plusieurs façons pour étudier la géomorphologie d'une région sont présentées dans ce rapport. Un modèle numérique qui prend en compte les phénomènes de diffusion et d'érosion / déposition par chenalisation a été codé en IDL (Interactive Data Language). Ce modèle a été appliqué dans la péninsule d'Eyre dans l'état d'Australie du Sud, où se trouvent plusieurs récents escarpements de faille. Cette utilisation du modèle a permis de déterminer les meilleurs valeurs pour les coefficients de diffusion pour chaque escarpement de faille.

La seconde partie de cette étude a été axée sur la région de Lac Eyre, un des plus grands bassins à drainage interne du monde. Une étude précise du paléolac de Billa Kalina et de ses environs a permis de déduire l'évolution du paysage dans cette région. Il semble qu'une significative subsidence s'est produite dans la région de Lake Eyre depuis le Miocène supérieur / Pliocène inférieur. L'hypothèse d'un mouvement descendant dans le manteau sous cette région est émise.

Acknowledgements

I first would like to thank my fantastic supervisor, Mike Sandiford for his warmhearted welcome, for all I learnt during this internship, for giving me the love of IDL, for making me believe in the Australia tilting and so much other things.

This internship would not have been possible without Julien Célérier who introduced me at Mike Sandiford and I am highly grateful for being confident in me.

Many thanks to all people of the Earth Science School of the University of Melbourne for this friendly and easy-going atmosphere at work, particularly to Sara Jakica who had to learn a new language : the "frenghish".

I warmly acknowledge the field-trip team, Mike Sandiford, Mark and Jeff Quigsley, Megan Weatherman, Ben McCormack, Sara Jakica and the pumpkin for all the good time spend with them in South Australia.

I also thank Kim Ely for introducing me to laboratory geology and exciting mineral hand-picking.

Special thanks to Mike and his family for being my Australian family and all my friends for their support and make me discover the Australian life.

Finally, grateful thanks to my mother who took care of my horses despite a big tiredness and had so much courage to fight.

Sequence of my internship

This research internship has been carried out from March to August 2006 within the School of Earth Science of the University of Melbourne, as part of the first year of my Master Degree in Earth Sciences. The initial subject of this internship concerned Timor collision zone and should include a field trip of 5 weeks in Timor. Unfortunately big troubles happened and it was too dangerous to go in Timor as previously organised. In May, my topic changed for being : "Tectonic geomorphologic studies in South Australia" and 3 weeks of field trip were spend in Whyalla and Lake Eyre regions in June 2006.

During this internship, I learnt a lot but unfortunately, the loss of time with the changement of topic at the middle of my internship didn't enable me to really use the model I write. That's why I cannot present a lot of results but I'm sure that all I learnt during this experiment is an important step in my career. In fact, I learnt how to code a geomorphologic model, how to use ENVI and Google Earth, the Tertiary geology of a big part of South Australia and of course, how to express myself in english.

Introduction

Australia is considered to be a very stable continent but evidences of recent tectonic are common within it. For example, active deformation within the Flinders Ranges is characterised by seismogenic strain rates over the last 30 years estimated to be as high as 10^{-16} s^{-1} (C  lerier et al. 2005). The Flinders Ranges are one of the most active deformation zone and this area is characterised by high earthquake activity and relative young topography suggesting that tectonics is an important factor in the shape of the landscape (Sandiford 2003).

Understanding the landscape and its evolution is a key to evaluating just how the tectonic processes operate in a defined area.

The aim of this internship was to study the landscape evolution and particularly the geomorphological response to tectonic events, using several methods.

At first, a numerical model will be presented. This model will provide the basis for evaluating geomorphologic responses to a faulting event, using the field work of the Whyalla area. Finally, we will study the landscape evolution in a part of Lake Eyre region (particularly in the Billa Kalina basin) using field work and spatial data.



1 Numerical Modelling of geomorphological processes

Studying the geomorphological processes that shape the surface of the Earth is important for understanding landscape evolution. Mass redistribution by erosion and sedimentation play an important role in shaping the surface and much work has been devoted to the modelling of landscape evolution (Tucker & Whipple 2002, Howard et al. 1994, Braun & Sambridge 1997). Landscape evolution modelling is a very useful tool in geomorphology because it allows the study of the influence of different parameters like the tectonic activity, the climate (by the quantity of precipitation) or the rock erosion properties, in the expression of geomorphological processes at the surface of the Earth.

During this internship, a simple geomorphologic model was developed using the IDL software. IDL allows the development of algorithms, interface and visualisations using the object-oriented programming methods.

In this part, the model is described, explaining firstly the modelled processes following by a description of the implementation.

1.1 Modelled Processes and equations

The developed model is a large-scale model in which it is assumed that the landscape evolution is controlled by two major processes : short-range or hillslope processes and long-range channelled water flow, like in many geomorphological models (Beaumont et al. 1992, Braun & Sambridge 1997, Chase 1992, Tucker & Whipple 2002). It is assumed that material transfer at the surface of the Earth dominated by the fluvial erosion are the result of interaction between hillslope and river processes (Lague 2001).

Rivers are organised in hydrographic network and transport the sediment load from erosion area to the network's outlet. River erosion is a function of the amount of water, the sediment load and the local slope.

In contrast, hillslope erosion occurs by a diffusive process with the consequence that the transport of sediment in this zone is very localised. In the following part, these two kind of transport will be precisely described and in particular the corresponding equations.

1.1.1 Short-Range Transport

The short-range transport or hillslope processes group principally weathering, slope wash, mass wasting and soil creep (Braun & Sambridge 1997).

The hillslope processes are known to vary with climatic conditions (vegetation, precipitation, temperature,...), rock's nature, tectonic context and anthropic factors (Selby 1993).

In order to model short-range transport, it is important to define a simple evolution law which integrate all of this processes.

The most widely used model is a simple diffusion problem in which the rate of change of landscape topography is proportionnal to the second spatial derivative of topography. The same approach was used in several models (Braun & Sambridge 1997, Howard et al. 1994, H. Kooi 1994)(equation 1).

$$\frac{\partial z}{\partial t} = k_s \nabla^2 z = k_s \frac{\partial^2 z}{\partial x^2} \quad (1)$$

where k_s is the landscape diffusion coefficient, z is elevation and x the horizontal distance. The landscape diffusion coefficient has a typical of $0.3m^2.yr^{-1}$ according to Braun & Sambridge (1997). Otherwise, Andrews & Hanks (1985) use a nominal diffusivity coefficient of $\kappa = 10^{-3}m^2/yr$

While this equation does not enable reproduction of the exact shape of many natural hillslopes

(Lague 2001), it has been shown to be adequate to model large-scale geomorphic systems (Tucker & Whipple 2002).

1.1.2 Long-Range Transport

Two general end-member types of long-range erosion laws are considered in most of geomorphological models : detachment limited and transport limited. The detachment limited family of models assume that rate of stream incision depends only on local bed shear stress. The transport limited models assumes the sediment flux is equated with the local transport capacity such that the rate of channel erosion (or deposition) is controlled by along-stream variations in transport capacities (Tucker & Whipple 2002, Lague 2001).

As in many models (Braun & Sambridge 1997, Beaumont et al. 1992), I have used a transport limited model.

The channel carrying capacity is computed from the local slope and the water discharge, as indicated in the equation 2 :

$$q^e = k_f \cdot Q^m \cdot S^n \quad (2)$$

where q^e is the channel carrying capacity, k_f the long-range fluvial material transport coefficient, Q the local flux of water and S the local downstream slope. The erosion law depends of the values of the powers m and n and it has been shown that the ratio $\frac{m-1}{n}$ should be between 0.3 and 0.7 (Lague 2001). In our model, a ration of 0.3 has been choose ($m=1.3$ and $n=1$) .

The long-range material transport coefficient has a typical value of $0.03m.yr^{-1}$ (Braun & Sambridge 1997).

Then, the channel carrying capacity is compared to the sediment flux q , which results from upstream erosion. We assume that the river transports less that its fluvial capacity and according to Braun and Sambridge (1997), a characteristic reaction time is used for computing the sediment load, like in the equation 3.

$$\frac{dq}{dt} = \frac{q^e - q}{t_{e,d}} \quad (3)$$

where $t_{e,d}$ is the characteristic reaction time.

Assuming that over an interval of time Δt , there is no local change in sediment load, the local change in topography can be expressed as the following equation 4 (Braun & Sambridge 1997):

$$\frac{dh}{dt} = -\frac{q^e - q}{L_{e,d}} \quad (4)$$

where $L_{e,d}$ is a length scale characterizing erosion/deposition processes. Then two situations can be considered :

1. When $q^e > q$ then $\frac{dh}{dt} < 0$, the sediment flux resulting from upstream erosion is smaller than the carrying capacity and erosion takes place and the change in the local topography is :

$$\frac{dh}{dt} = -\frac{q^e - q}{L_e} \quad (5)$$

where L_e is the length scale for erosion processes.

2. When $q^e < q$ then $\frac{dh}{dt} > 0$, the carrying capacity is smaller than the sediment flux and deposition takes place and the change in the local topography is :

$$\frac{dh}{dt} = -\frac{q^e - q}{L_d} \quad (6)$$

where L_d is a length scale for the deposition.

1.2 Implementation

1.2.1 Background

Firstly, we define a landscape which has to be discretized as a finite number of nodes. In this model, we use a regular mesh grid as represented in figure 1.

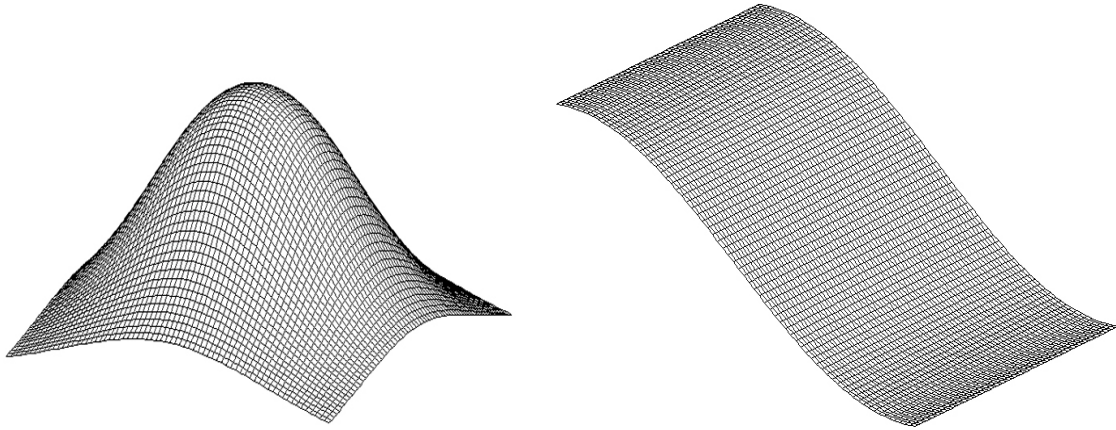


Figure 1: Two Examples of simple surface meshed in a regular grid

When this initial topography is defined, there is a user defined number of loop and each loop is in fact a succession of several procedures which correspond to several processes as is indicated in the following enumeration :

1. Computing the precipitation
2. Calculating the Flow of water
3. Short-Range transport
4. Long-Range transport
5. Graphic representation and exportation

A description of every process is provided below.

1.2.2 Description of a loop

Precipitation

Precipitation is representing by an array of the same size as the surface and a defined water quantity is attributed at each node.. This procedure is included in the loop because it allows to represent some variations in precipitations (climatic change) in modifying the quantity of rain in respect with the timestep.

Flow routing

This procedure define if the water attributed to each node by the precipitation procedure is in a stable state and then should stay at this node or, on the contrary if the water should flow to an other node. For computing a "bucket passing" algorithm was developed. This consists of ordering all the nodes by elevation from the highest to the lowest, then finding for each node the lowest elevation adjacent neighbour (when the gradient is maximum). Water is passed from the node to the receiver neighbour.

We consider that all precipitation is assumed to traverse the landscape with a charactertic timescale much shorter than the computational timestep. The cumulative quantity of water which was passed across each node defines the local flux of water (Q in the equation 2).

Resolving the short-range transport equation

We used an explicit formulation for computation of the short-range transport (equation 1). This simple resolution demands the use of small timestep for complying with stability condition. However, because geomorphic processes act on time scales of the order of 10 to 100 years, numerical simulations of landscape evolution necessarily require such a very fine temporal discretization (Braun & Sambridge 1997), which is compatible with an explicit resolution.

The equation 1 can be simplified in a discret temporal resolution like the following equation :

$$\Delta z = \Delta t \cdot \nabla z \cdot k_s$$

where k_s is the , ∇z the slope, Δt the timestep and Δz the variation of elevation. For computing this resolution, the model calculate the gradient between each node and all of its neighbours and derives the value of the variation of elevation for each node. At the end of the short-range procedure, the variable which represents the ground is actualised in function of the variation of elevation in each node.

Resolving the long-range transport equation

The local slope and water discharge define the channel carrying capacity (Beaumont et al. 1992, H. Kooi 1994). According to equation 2, the relative values of the sediment flux Q^i and the fluvial carrying capacity Q^e determine if the river is depositing or eroding,

The elevation is updated from :

$$h_i = h_i + (Q^i - Q^e)$$

where h_i is the elevation at the node i , Q^e the fluvial carrying capacity and Q^i the sediment flux.

Graphics Representation and Output

Results are represented with graphic representations and the array of elevation is exported in a .txt file.

The graphic representation allows visualisation of the surface as shown by the figure 2.

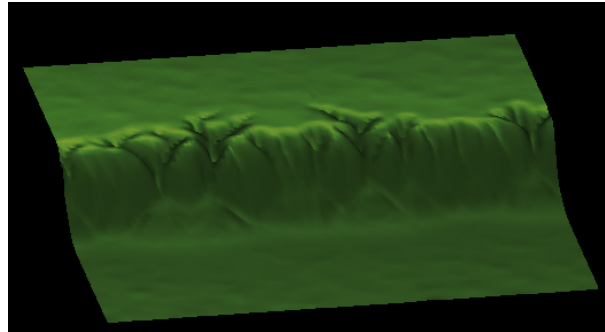


Figure 2: Example of graphic representation of the surface, result of the modelling

Furthermore, profiles across the scarp are done and allow study of diffusive processes by comparison with diffusive profiles from the field work (figure 3).

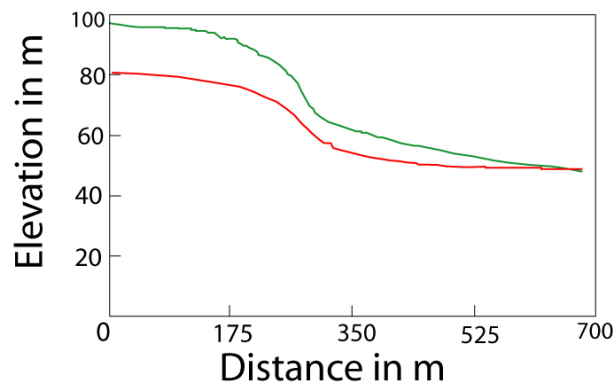


Figure 3: Example of graphic representation of a diffusive profile across the scarp. The red curve is the modelling and the green curve is the GPS data curve.

The .txt file which contains elevation values resulting of the modelling can be open with the software ENVI which allows a precise study and more particularly of the fluvial processes.

1.2.3 Why IDL ?

The surface process model defined by equations 1-6 has been coded in the Interactive Data Language (IDL) which allows the object orientation programming. This kind of programming represents a powerful tool for developing a geomorphologic model because it enables the individualisation of each function or procedure and then an easier possibility to separate processes applied during one simulation.

The Interactive Data Language (IDL) is a proprietary software system distributed by Research Systems, Inc., of Boulder, CO (<http://www.rsinc.com>). IDL grew out of programs written for analysis of data from NASA missions. It is therefore oriented toward use by scientists and engineers in the analysis of one-, two-, or three-dimensional data sets.

In fact, IDL is a computer language which offers all the power and programmability of a high level language like FORTRAN or C and adds other capabilities like interactivity, graphic display and array-oriented operations. Some characteristics of IDL are optimized array-operations, rapid responses and iterations, easy operations with data structures and possibility to do object-oriented programming.

The idea behind object-oriented programming is that a computer program may be seen as comprising a collection of individual units, or objects, that act on each other, as opposed to a traditional view in which a program may be seen as a collection of functions, or simply as a list of instructions to the computer. Each object is capable of receiving messages, processing data, and sending messages to other objects.

The association between flexibility and easily coding method is powerful for programming.

2 Geomorphologic response of a faulting event

The existence and forms of fault scarps provides an important insight into past history of surface-rupturing earthquakes.

Wallace (1977) noted that strictly measures of geomorphology could yield information on relative ages, "other things" being equal. Buckman & Anderson (1979) formalized this relation with plots of scarp height versus scarp slope angle.

Hanks et al. (1984) examined the applicability of the one dimensional diffusion equation with constant coefficient to the morphology of different geologic structures across a wide range in age (3 to 400 000 ky before present), scarp height (1 to 50m) and tectonic circumstance.

Subsequently, Andrews & Hanks (1985) developed a procedure to invert a scarp diffusive profile to find its "diffusion age" which can be correlated with the absolute age using the diffusion coefficient.

During this internship, this idea of utilize diffusive profiles across the scarps has been applied to young fault scarps from Whyalla in South Australia.

2.1 Area of study : Whyalla's scarps

The area of study is located between the latitudes 33° and $33^{\circ}30'$ and the longitudes 137° and $137^{\circ}30'$, in the Eyre Peninsula (figure 4) in South Australia.

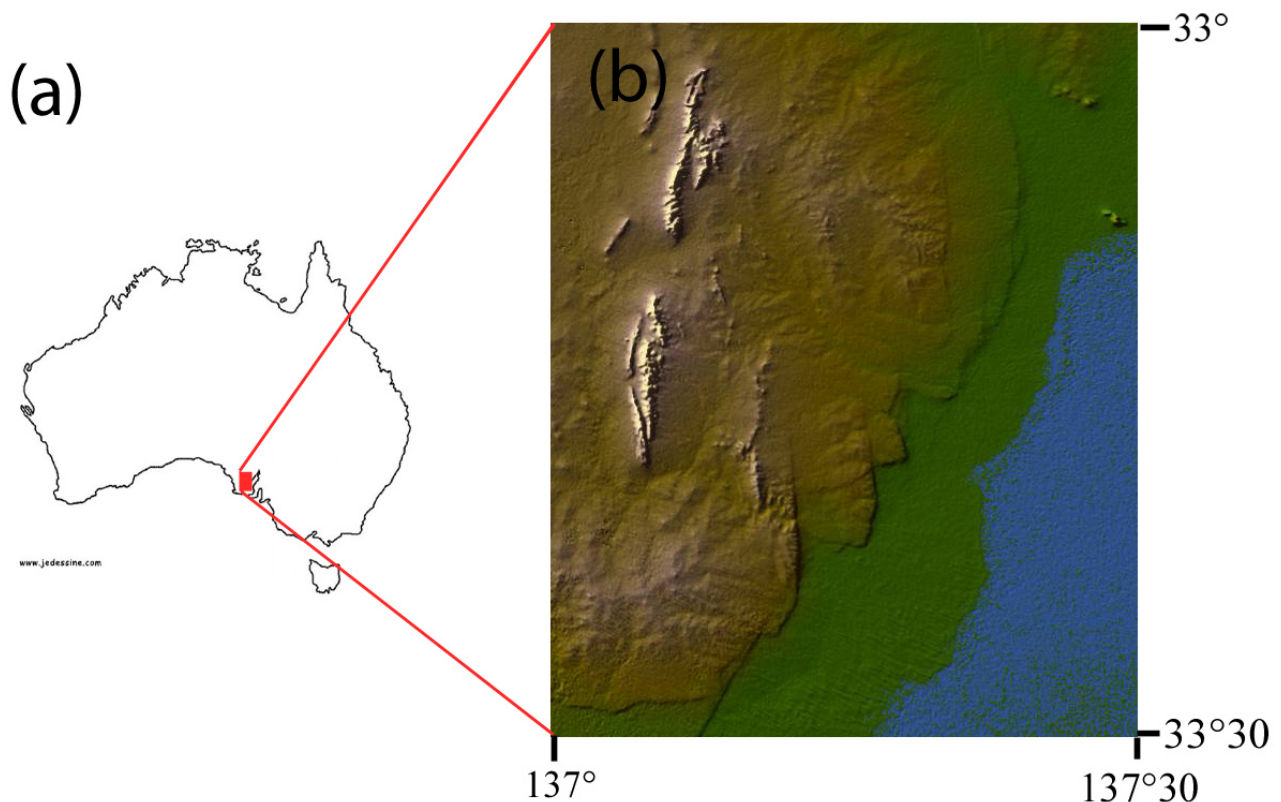


Figure 4: (a) Localisation of the Eyre Peninsula in Australia and (b) SRTM image of the area of study, showing the Whyalla's scarps

In this area, the landscape is principally characterised by a gently undulating surface of low relief. This area seems to have been subject of some extremely long period of slow erosion which has continued up to geologically recent times (Miles 1951).

However, the landscape is interrupted by a system of North-South scarps which faces exclusively to the east.

For convenience of description and identification of these scarps, names used by Miles (1951) are conserved as shown on the following map (figure 5)

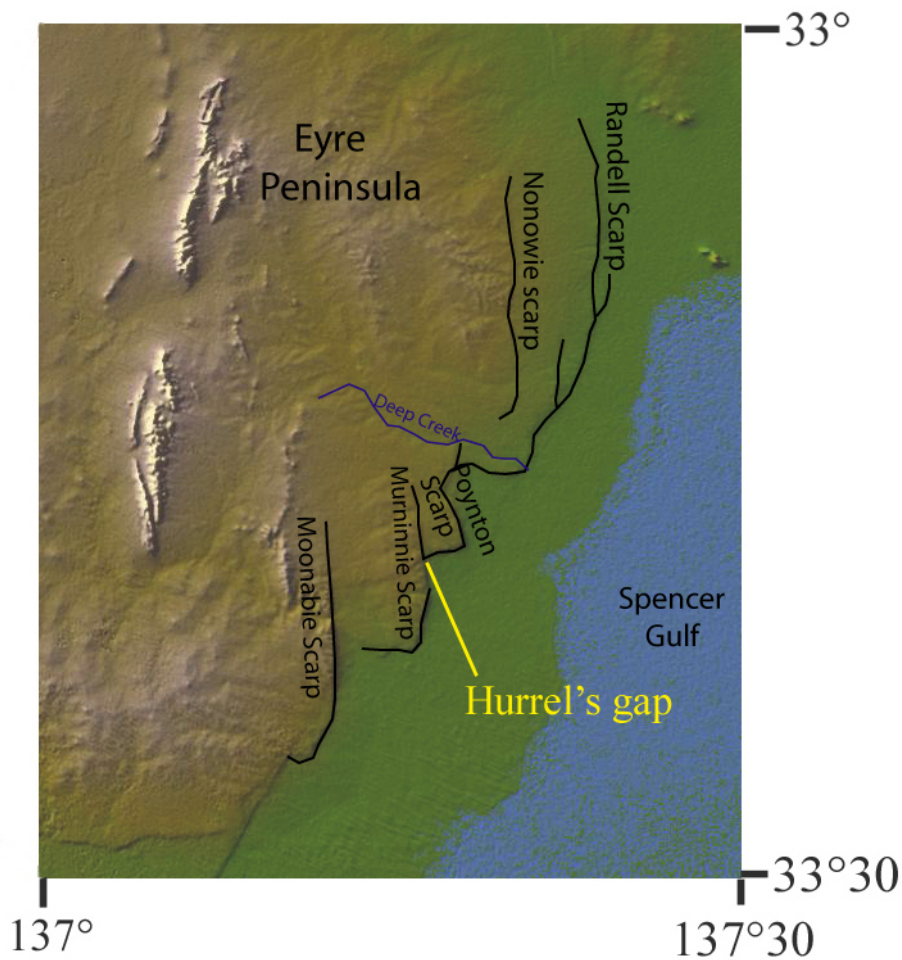


Figure 5: Part of Northeastern Eyre Peninsula showing North-South Fault Scarps (Miles 1951).

Because of their exceptional linearity, Jack (1914) and Miles (1951) have interpreted these scarps as fault scarps. An alternative explanation is that some of them form coastal features associated with marine erosion and a growth of reefs. For example, Dunham (1992) suggests that the Poynton scarp can have a reef origin. We studied two particular scarps : the Randell scarp and the Murrinnie scarp where there is little doubt that these are not fault scarps as indicated by observations discussed below.

2.1.1 Murninnie scarp

This scarp rises 40m above the adjacent plain and extends approximately 7km south of Hurrel's Gap (figure 5). The old Murninnie copper mine at the Hurrel's gap exposes a reverse fault in the mine entrance (figure 7). This fault uplifts basement rocks (mylonite) above Tertiary sediments (white clay) along a fault plane that trends 175°N and dips 45°W . As this fault trace is coincident with the scarp, there is little doubt the Murninnie scarp is not a fault scarp.



Figure 6: Exposure of the reverse fault at Murninnie scarp at the entrance of the copper mine.

2.1.2 Randell scarp

The Randell scarp extends for approximately 20km in a N-S direction and it is an about 20m-high scarp. It is quite steep but has clearly been subjected to greater fluvial incision than the Murninnie scarp.

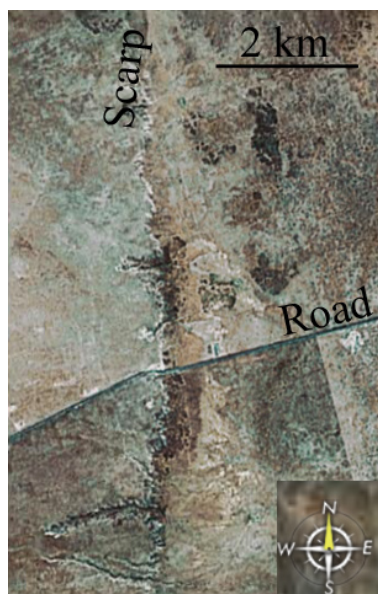


Figure 7: Google Earth image of the Randell scarp showing the fluvial incision.

2.1.3 Age of the Faulting

In South Australia, Flinders Ranges area presents an important distribution of seismicity (figure 8). Some events are localised in the Eyre Peninsula.

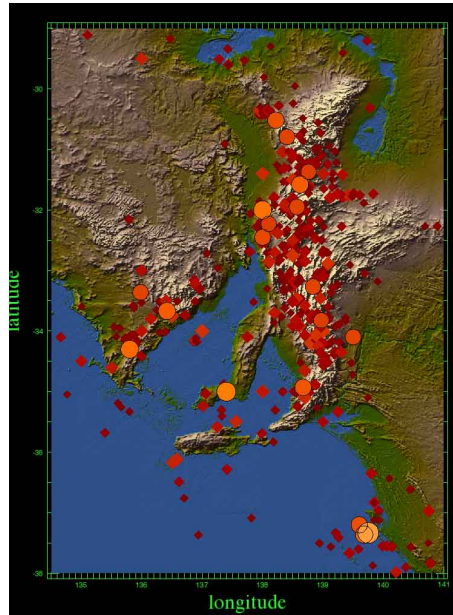


Figure 8: Distribution of seismicity ($M > 3$) in the Eyre Peninsula area from Geoscience Australia data.

There is ample evidences that the fault scarps of the Whyalla area are relatively youthful features (Miles 1951). Constraints of the age of the faulting are not very defined but some evidences give a possible age interval.

Firstly, at the Randell scarp, Miocene limestone and Pleistocene colluvium are faulted, implying that fault must be younger than Pleistocene (younger than 1.8 Ma).

A recent paleoseismicity study along the Roopena fault was done by Crone et al. (2003). The scarp associated with the Roopena fault is approximately 30km-long in the N-S direction and localised 5km North of Randell scarp and about 40km NE of Murninnie scarp.

Because of the similar N-S trending and localisation of these scarps, we consider that these scarps are the results of the same tectonic phase. Then, it is possible to have a constraint on the age of faulting in this area thanks to the paleoseismicity study along the Roopena fault. Crone et al. (2003) used stratigraphic data, OSL ages estimates and structural relations in trenches to define consistent Quaternary paleoseismic history of the Roopena fault. The interpretation of surface rupturing on the Roopena fault is (1) the most recent event occurred about 27-30ka and (2) a penultimate event occurred about 100ka. The height of the scarp along the Roopena fault is about 3.8m and results of two events since 100ka. Then, we decide an average growing of the scarp height of 1.9m per 50ka.

The Murninnie scarp is a 35m scarp then an age of 975 000 years for the first faulting event is inferred.

The height of the Randell scarp is about 20m then the age of the first surface rupturing faulting event should be about 525 000 years.

There is large incertitudes on these ages but they can give an idea of the age of the beginning of the faulting. These values have been used for our modelling.

2.2 Field Methods and collected datas

2.2.1 High resolution GPS

During the field work, a DGPS (Differential Global Positioning system) using 'Omnistar' Satellite correction service was used. A DGPS is a method of improving the accuracy of the receiver by adding a local reference station to increase the information available from satellites. Omnistar provides one of the most accurate positioning services available. System errors, such as orbit, timing and atmospheric errors limit the accuracy that can be achieved using the US Global Positioning System Satellite service.

The Omnistar system is a global real-time differential GPS broadcast system delivering corrections from an array of base stations positioning throughout the world.

Omnistar uses a network of reference stations to measure Ionospheric interference and other errors inherent in the GPS system. The omnistar correction data is transmitted to the user and permits an accuracy of approximately 1m.

2.2.2 Profiles of the scarps

Using previously described DGPS system, we did several high precision cross-sections across the scarps.

Some cross-sections were done across hillslope and provides quasi-diffusive profiles (figure 9).

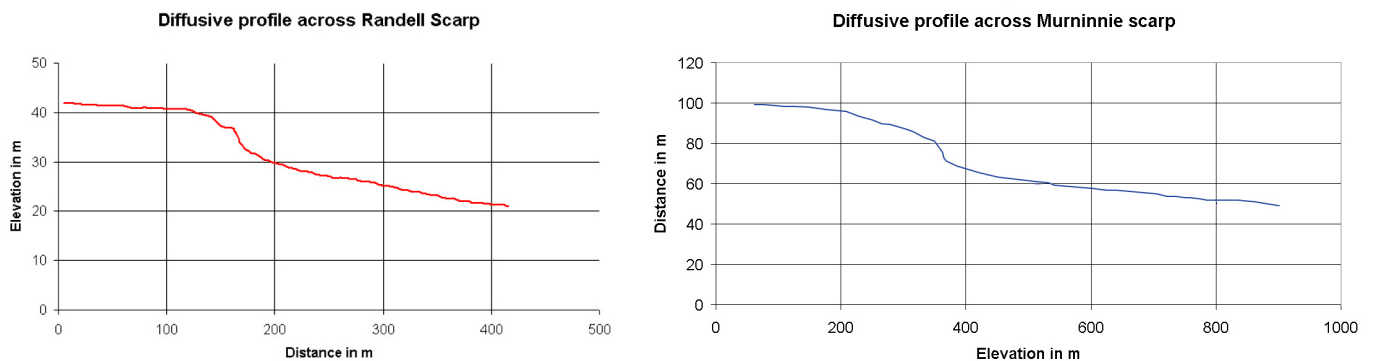


Figure 9: Collected GPS data showing two diffusive profiles across the Randell scarp and the Murninnie scarp

Unfortunately profiles collected along river channels could not be used during this internship because of the lack of time after the field trip. The comparison between morphology of the scarps and results of the modelling was only applied for diffusive profiles.

2.3 Modelling the diffusive response faulting events

A procedure in the model can read diffusive profiles of the scarp and an inversion method allows to find the best diffusivity coefficients for each scarp. Few studies give some value for these empirical coefficients and the fact of correlating the model with data from field work enable the quantification.

Every modelling need to consider two different diffusivities between the initial rock and the sediments which result from the diffusive processes. An important aspect is to have the ratio between initial rock and sediments diffusive coefficients.

2.3.1 Murninnie scarp

As showed before, the estimate age of the Murninnie scarp in function of its height is about 975 000 years. With this estimate age, results of the modelling of diffusive processes are shown in the figure 10. For having the best concordance between modelling and data, diffusive coefficient used are 8.10^{-4} for the diffusivity of initial rocks and 0.015 for the diffusivity of the sediments from the diffusion process.

In this case, the diffusivity of the sediments is 18.75 times higher than the diffusivity of initial rocks.

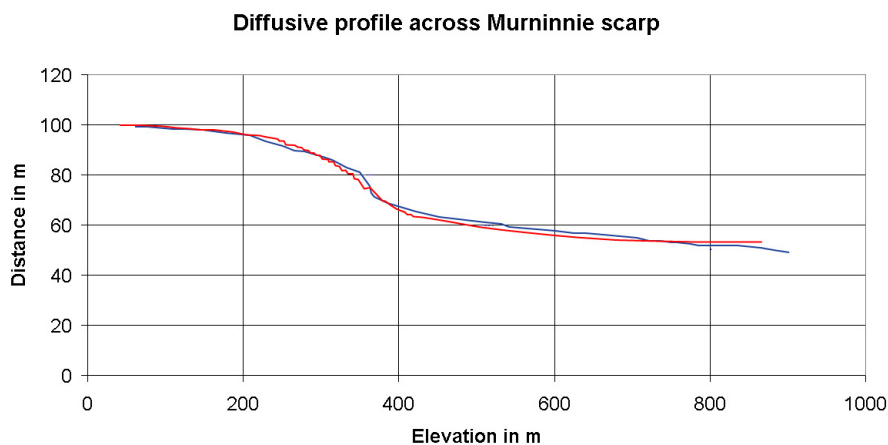


Figure 10: Results of the Murninnie scarp modelling : the two curves show the best fitting between modelling (red curve) and data (blue curve)

2.3.2 Randell scarp

The estimate age of the Randell scarp is about 525 000 years. The results of the modelling for the Randell scarp indicate diffusivity coefficients of 5.10^{-4} for the initial rock and 0.01 for the sediments from diffusion processes (figure 11). In this case, the ratio between diffusivity of the sediments and the initial rock is 20.

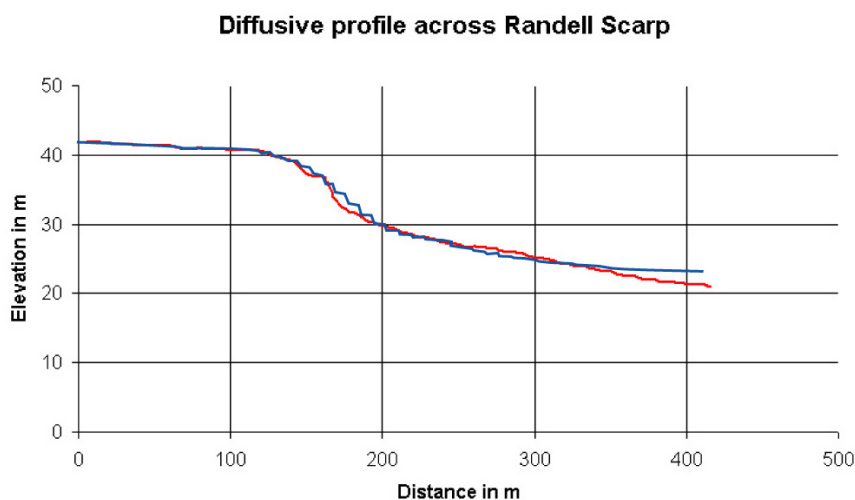


Figure 11: Results of the Randell scarp modelling : the two curves show the best fitting between modelling (blue curve) and data (red curve)

2.4 Interpretations / Conclusion

It is instinctive to have a higher diffusivity coefficient for the sediments from diffusion processes than for the initial rock. It looks like ratio between diffusivity of sediments from diffusion processes and initial rocks has a value close to 20. However, studies of other scarps can help to determine if it is a coincidence or on the contrary a general relation.

An other interesting point is that diffusivity of basement which is uplifted at the Murninnie scarp is higher than the diffusivity of Tertiary sediments uplifted at Randell scarp. It is possible to imagine that fracturation in basement rocks increase the diffusivity of the rock. As for the precedent example, more studies of other scarps is required to conclude with confidence.

These presented studies should be see as an example of using the modelling to understand geomorphologic processes and to quantify coefficient which defines the diffusivity of this rock in a particular case.

3 Landscape Evolution in Billa Kalina Area

The third part of this report presents different tools for studying landscape evolution, based on field work and spatial data in the region of the Billa Kalina basin and southern Lake Eyre basin, in South Australia.

We bring more interest in some of the Tertiary basins which can be divided in two main groups in South Australia :

- Non-marine basins, to the North, where the sediments are relatively thin and characteristic of fluvial or lacustrine environments (Lake Eyre, Billa Kalina, Torrens or Hamilton basins).
- Marine basins to the South where the sediments are accumulated in passive continental margin basins and the deposition of considerable thickness of marine sediments is a consequence of the initiation of marine transgressions, resulting from the separation of Australia from Antarctica. (Alley & Lindsay 1998). (Murray, Eucla, Saint Vincent and Gambier basins).

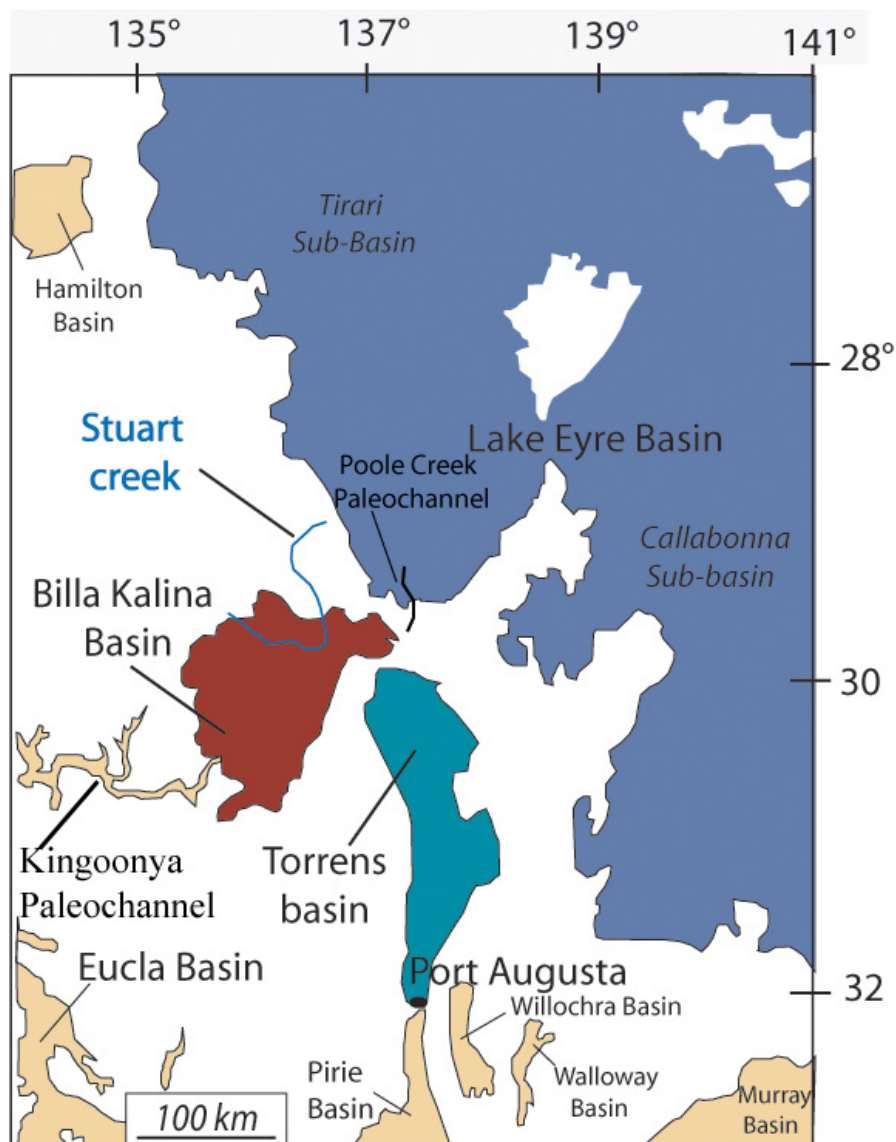


Figure 12: Distribution of Tertiary basins in the northern part of South Australia

In fact, Lake Eyre, a great salt lake, is one of the largest areas of internal drainage in the world. The lowest part lies 16m below sea level (SRTM data). Lake Eyre seems to be close to the centre of a very large near circular topographic depression as we can see in figure 13 :

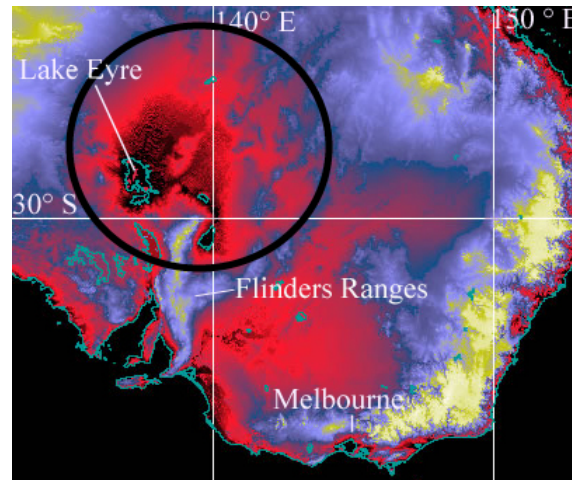


Figure 13: Elevation map around Lake Eyre basin showing the very large near circular topographic depression mentioned in the text.

One very interesting observation is that there is no marine tertiary sedimentation in the Eyre basin. In fact, lowest ranges south of Lake Eyre culminate at about 80m above sea level whereas the sea level was higher during most part of the Tertiary (Haq et al. 1987) (figure 14).

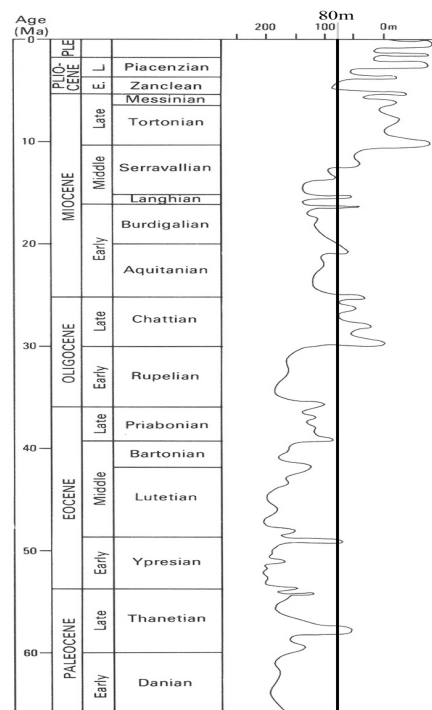


Figure 14: Tertiary sea level curves (Haq et al. 1987). The line at 80m corresponds at the elevation of the lowest ranges South of Lake Eyre.

Even more surprising is that further West along the Eucla basin, Tertiary limestones are found at elevations up to 300m above sea level (figure 15).

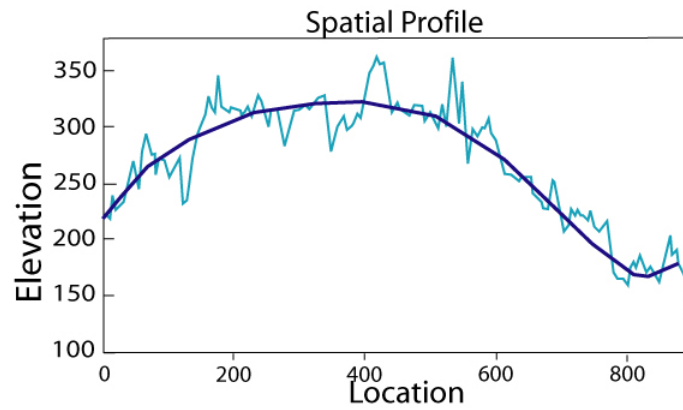


Figure 15: Elevation of Eocene sediments of the Eucla basin and the trend curve is in dark blue

This section focuses in the question of why Lake Eyre Basin has not been flooded during the Tertiary. What did arrive to the landscape to explain these titlting ? The following part presents the study which was carried out in the Billa Kalina area and focuses only about the Eyre basin.

3.1 The Billa Kalina Basin

The Billa Kalina basin refers to sediments deposited in an enclosed basin situated between the Eucla basin paleodrainage network and the Lake Eyre Basin. This area is between latitudes 29°30S and 30°50S and longitudes 135°0E and 137°30E, 600km NNE from Adelaide in the arid central region of Australia (figure 12). The covering area of Billa Kalina basin is about 18 000 km².

In the following part, we will firstly present the stratigraphy of Tertiary sediments in the Billa Kalina basin following by a sedimentologic and geomorphologic study.

The geological map (figure 16) was carried out from four 1:250 000 geological maps (Cowley & Martin 1991, Johns et al. 1966, Krieg et al. 1991, Ambrose & Flint 1980).

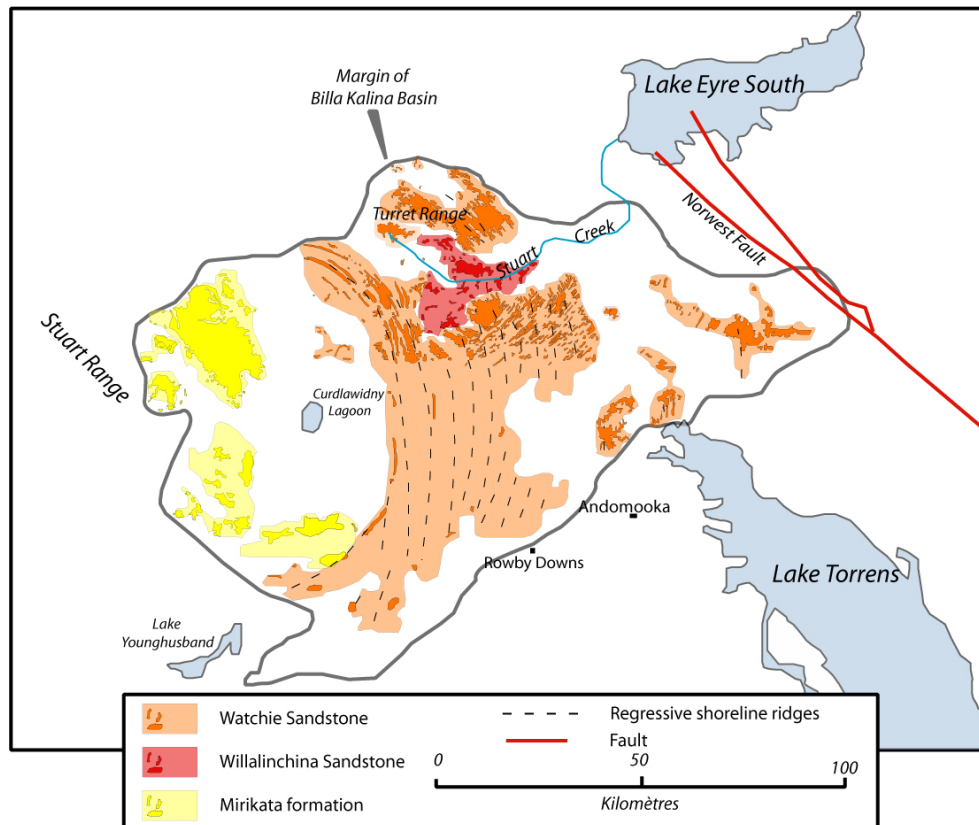


Figure 16: Geological map of the Billa Kalina basin. Transparent colors are interpolation whereas dark colors are outcrops

3.1.1 Stratigraphy

The Billa Kalina Basin is constituted by a thin, flat lying succession of Tertiary age sediments (Alley & Lindsay 1998). Three main formations are considered in this basin : the Mirikata formation, the Watchie sandstone and the Willalinchina sandstone. (Ambrose & Flint 1980, Krieg et al. 1991).

Mirikata Formation

The Mirikata Formation is a clay-dolomite succession restricted to the western part of the basin (figure 16). This unit is divided in three main formations (Alley & Lindsay 1998).

1. The Danae conglomerate is a thin basal conglomerate layer comprising resistant silcrete and Permian rocks clasts in a fine to coarse grained matrix.
2. The Billa Kalina Clay member is a 4-6m thick yellow and gray clay.
3. The Millers Creek dolomite member is up to 10m thick and comprises dolomite or dolomitic limestones.

In Millers Creek Dolomite, the presence of fresh water molluscs indicates a lacustrine origin and permits the determination of a Early to Middle Miocene age in Millers Creek Dolomite. The contacts Millers Creek Dolomite member/Billa Kalina clay and Billa Kalina clay/Danae conglomerate are gradational then we infer that the Mirikata Formation is Early to Middle Miocene (Krieg et al. 1991).

The Danae conglomerate is interpreted to be largely colluvial and talus slope sediments whereas Millers Creek Dolomite and Billa Kalina clay are interpreted lacustrine deposits (Ambrose & Flint 1980).

According to (Cowley & Martin 1991), the Millers Creek dolomite member is an evaporitic dolomite and results to the drying of Lake Billa Kalina.

Watchie Sandstone

The Watchie sandstone is an uniform layer of sandstone and silstone and this formation is regarded as a regressive lacustrine fluvial succession (Ambrose & Flint 1981).

This formation is constituted of a basal 10cm-erosive breccia with reworked Bulldog shale, overlain by about 3m thick very fine to fine-grained white sandstone and silstone interbedded.

The upper part of the Watchie sandstone is a widespread yellow fluvio-lacustrine sandstone and contains upward coarsening sequence.

The white sandstone is interpreted to have been deposited during a transgressive lake phase, locally in channels (Callen 1981). The upper yellow sandstone is distributed in a serie of concentric arcuate ridges and interpreted as a regressive strandline sequence.

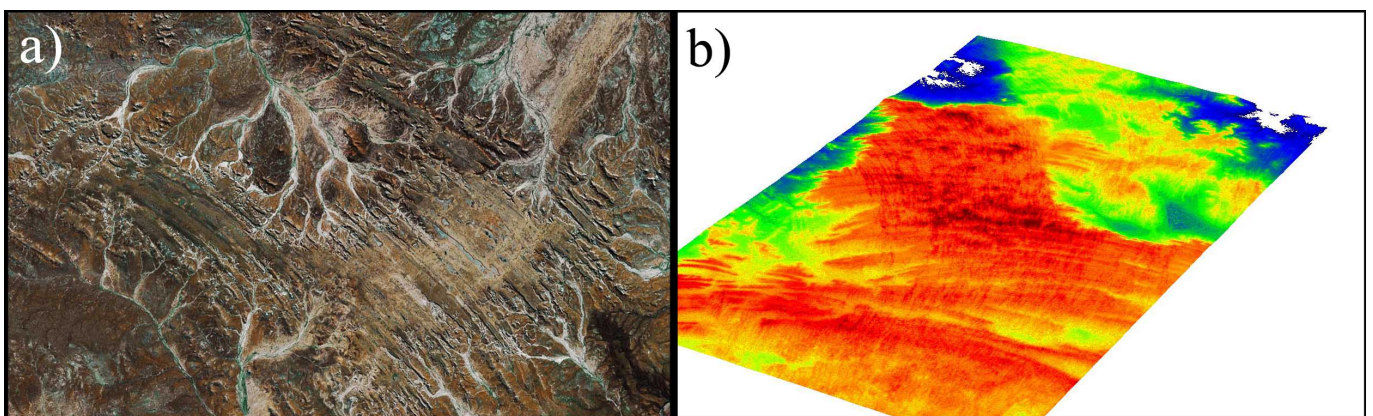


Figure 17: Beach ridges in the Watchie Sandstone a)Google Earth Image b) SRTM data represented with ENVI (vertical exaggeration=20)

Around Millers Creek plateau, the lacustrine deposits of Millers Creek Dolomite and Billa Kalina Clays, the circumference of the strandlines are concordant with the lacustrine deposits of Millers Creek Dolomite and Billa Kalina Clays which agree with a genetic connection between this two formations (Ambrose & Flint 1981). In addition, the top of the arcuate ridge system

and the top of the Millers Creek dolomite Member together define a concordant surface at 110-130m elevation, with a very gentle southward dip (Cowley & Martin 1991, Cowley 1990). The Watchie sandstone is probably of a Early to Middle Miocene, contemporary of the Mirikata formation.

Willalinchina Sandstone

The Willalinchina sandstone is a silicified quartz unit, up to 10m thick and restricted to the Stuart Creek region (Krieg et al. 1991). The sandstone is well known for its presence of abundant plant fossils (Ambrose & Flint 1981, Greenwood et al. 1981)

The basal layer is a thin layer (up to 80cm) of persistal conglomerate consisting of clasts of silcrete, quartz, feruginised Bulldog shale and sandstone, probably remains of paleovalley incision.

This layer is overlain by 7-9m of strongly silicified white sandstone in which leaf impressions and casts, ripples and cross-bedding are well preserved (figure 18).

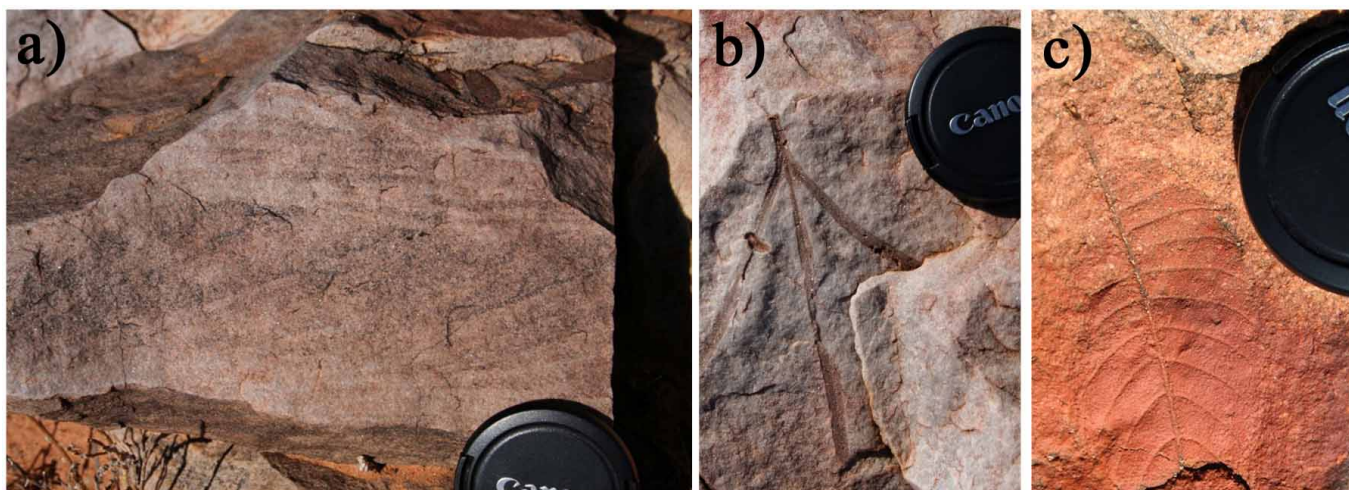


Figure 18: The channel sediment of the Willalinchina Sandstone. a) cross-bedding, b) and c) leaf impressions

The fossil-rich sandstone of the upper unit is considered to have been deposited in low energy water environment (Greenwood et al. 1981). The deposition probably started with seasonal flood and basal conglomerate lags were deposited during initial water level rise in the paleovalley (Zang et al. 2006).

Two hypothesis are considered for the age of this formation. Several authors think that there is floristic similarities between Stuart Creek macroflora and those of the Middle Eocene sites of the Poole Creek paleochannel (figure 12) (Greenwood 1996, Christophel et al. 1992), then they consider the Willalinchina Sandstone as a Middle Eocene sandstone. On the contrary Zang et al. (2006) recently write : "The field observation suggests that the Willalinchina sandstone onlaps the Watchie sandstone and had been deposited in a paleovalley incised into the Watchie sandstone and basement Bulldog shale.". This observation suggests that Willalinchina sandstone is younger than Watchie sandstone. The Watchie sandstone is considered to be of an Early to Middle Miocene age, then the Willalinchina sandstone which characterised a fluvial incision phase of late Miocene or Early Pliocene.(Zang et al. 2006).

3.1.2 Sedimentologic and geomorphic features

In order to define the paleogeography in the Billa Kalina basin, several sedimentary features were observed during the field work and are described in the following part.

Strandlines in the Watchie Sandstone

Strandlines in the Watchie sandstone are indicators of the regression of the shallow part of the lake in which were deposited the Billa Kalina Clay and the Millers Creek Dolomite. In fact, the ridges are regular, the lithology is upward-coarsening which is consistent with a regressive lacustrine sequence (Ambrose & Flint 1981).

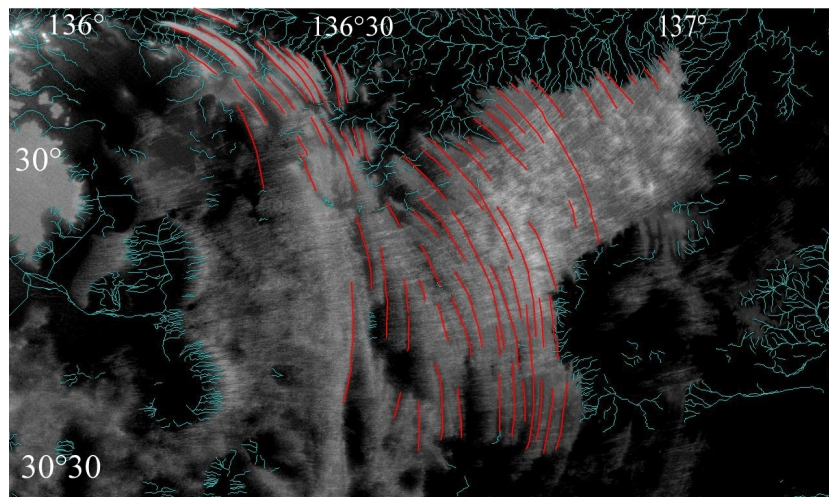


Figure 19: Beach ridges in the Watchie Sandstone SRTM data obtained in ENVI

Some authors attribute the strandlines to regression features which are consequence of climatic change and, in particular, the Milankovitch cycles.

During the tertiary, the period of the Milankovitch cycles was about 40 000 years. Calculating the number of strandlines can give an idea of the minimum regression period. In this case, at least 40 strandlines are evident (figure 19) which correspond to a minimum period of regression of 1.6 millions years. The vast distance over which the Lake was regressed and the quasi-uniform parallel development of strandlines implies a relatively stable flat land surface. However, around latitude $29^{\circ}55'$ and longitude $136^{\circ}35'$ there is a discontinuity within the strandlines (figure 20) which can be consequence of mild tectonics.

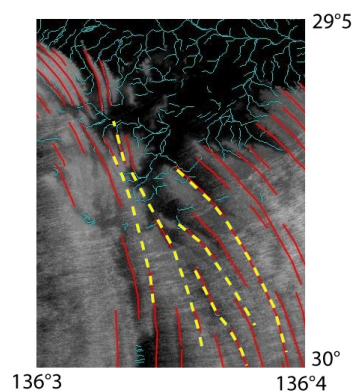


Figure 20: Zoom in the figure 19 where a discontinuity within the strandlines can be observed.

Close to Millers Creek plateau, the regression direction appears to be WSW whereas further East, this regression direction is SW. This observation can be an argument favorable for the hypothesis of uplift of southern margin of the Billa Kalina mentioned by Alley & Lindsay (1998).

Base of the Watchie Sandstone

Regression in a shoreline lake should occur in a relatively stable environment. We did a representation of the surface of the Watchie sandstone base in order to determine if this surface has been subject to tectonic events like faulting. If it was the case, the base of the Watchie sandstone formation should present discontinuities.

Using ENVI and the geological maps, points at the base of the Watchie sandstone base were collected and a IDL program was used to represent the base's surface of the Watchie sandstone (figure 21). The base of this formation is very slowly dipping towards E which is not in agreement with the direction of regression given by the strandlines orientation. This dipping suggests a tilting post-deposition of the Watchie sandstone with uplift at the South-West (Eucla Basin) and/or subsidence at the North-East (Lake Eyre).

The average elevation of the Billa Kalina basin is about 125m, but this was a closed lake so we cannot correlate this elevation with the sea level.

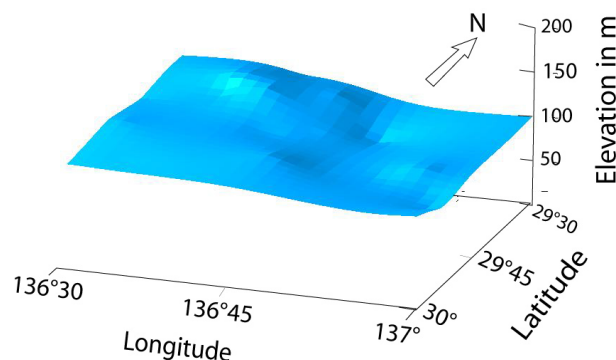


Figure 21: Base of the Watchie sandstone (representation with IDL programming) showing a slowly dip towards NE

Paleocurrents in the Willalinchina Sandstone

Outcrops of Willalinchina sandstone in Stuart Creek presents sedimentary features which are indicators of direction of paleocurrents during the deposition of the sandstone. During the field work, paleocurrents directions were collected and a rose diagramm was done. It indicates a NE direction (figure 22). This NE direction indicates a paleotransport towards Lake Eyre, then the Willalinchina sandstone was deposited in the drainage area of Lake Eyre during the Late Miocene or Early Pliocene.

3.1.3 Interpretations

All of these observations constraint the paleogeography and tectonic history of the Billa Kalina Basin.

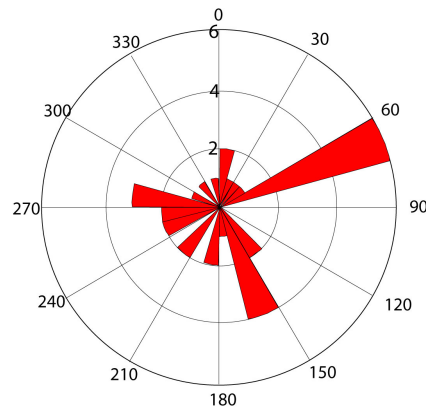


Figure 22: Rose diagram of the paleocurrents directions in the Willalinchina sandstone in Stuart Creek area which indicate a major N68 direction ($\pm 8^\circ$)

The beginning of the sedimentation in this basin is dated Early to Middle Miocene and corresponds to a paleolake which presents strandlines indicators of a regression towards WSW. A discontinuity within the strandlines suggests some mild tectonics during the Miocene. However, base of the Watchie sandstone is in disagreement with the regression direction given by the strandlines. This observation suggests tectonic movements (uplift of Eucla basin and/or subsidence at Lake Eyre and Lake Torrens) since at least the Early Miocene. Furthermore, fluvial sedimentation dated of Late Miocene/Early Pliocene indicates paleocurrents towards Lake Eyre. Subsidence of Lake Eyre region since the Late Miocene seems to be a concordant hypothesis.

3.2 Adjacent Basins

The interesting point is to replace Billa Kalina evolution in a bigger geological context and to understand the landscape evolution. As demonstrated before, the Billa Kalina Basin is consequent of a paleolake which extended on a surface of about 18 000 km² during the Early-Middle Miocene. Billa Kalina was a vast shallow lake and required a large flux of water in order to sustain it.

Billa Kalina lake should be associated with a very large drainage area whereas the paleolake is localised at the intersection of three basins and Ranges.

Stuart Ranges are at the North-west margin of Billa Kalina basin and represent a high topographic area which limits the extend of the Billa Kalina paleodrainage area. Uplift at Stuart Range is dated before and during Eocene (Alley & Lindsay 1998) before the filling of Billa Kalina Lake.

The Kingoonya paleochannel is localised at the SW of Billa Kalina Basin and indicates a mostly South-West direction of paleocurrents (Cowley & Martin 1991). This paleochannel belongs to the large paleodrainage area of the Eucla basin which includes Tertiary sediments deposited in marine and terrestrial settings in the southwestern part of South Australia. An extensive region of paleodrainage fringe the Eucla basin which has preserved alluvial and colluvial sediments. The Kingoonya paleochannel belongs to this region and sediments within the channel comprise two formations : (1) Pidinga Formation (Middle to Late Eocene) and (2) Garford Formation (Miocene to Pliocene)(Alley & Beecroft 1993, Pitt 1978, Alley & Lindsay 1998).

During the existence of Billa Kalina Lake, Kingoonya paleochannel was active and the paleodrainage of the lake could not be very extensive towards the South-West.

Furthermore, a precise observation of the strandlines indicates that it is not possible to fill Billa Kalina Lake if North of Lake Torrens and South of Lake Eyre were at the same elevation

than today. In fact, some strandlines are localised between South Lake Eyre and North Lake Torrens (figure 23). It is impossible to have a lake at this place without parts around higher. This implies a relative subsidence of Lake Eyre South and Lake Torrens since the Early-Middle Miocene. These two basins will be studied in the following part.

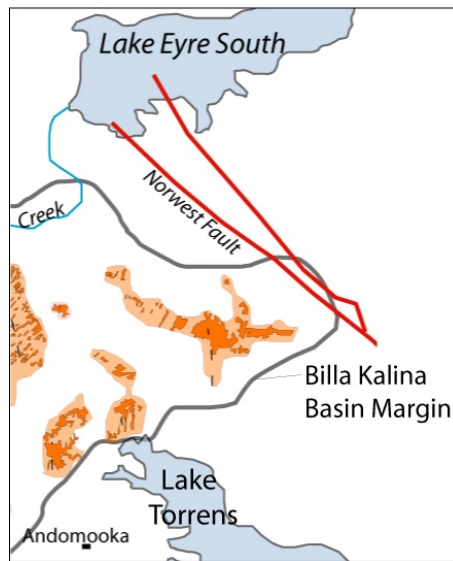


Figure 23: Zoom in the geological map of Billa Kalina basin in order to show the outcrop of Watchie sandstone close to the Eyre basin and the Torrens basin.

3.2.1 Lake Torrens

The Torrens basin is a north-south-trending structural depression where refraction seismic studies and drilling (figure 24) indicate locally complex structure and fault-controlled horsts and troughs along the eastern basin margin (ETSA 1989).

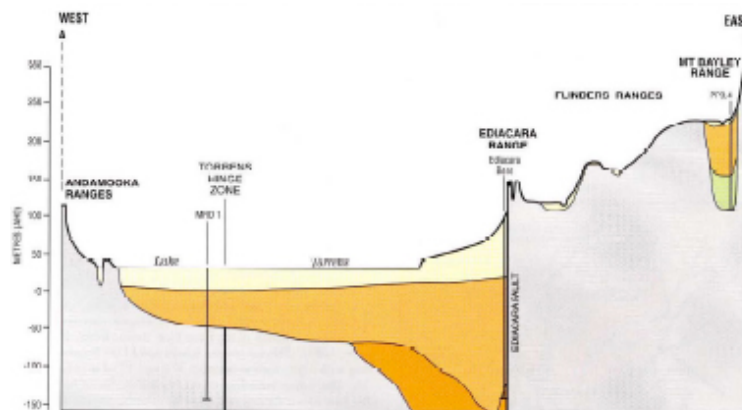


Figure 24: Cross-section trough Tertiary sediments in the Torrens basin

Miocene sediments in Torrens basin are regrouped in the Neuroodla Formation. The paleogeography associated with these sediments is low energy flood-plain with localised sand channels for the lower layer whereas upper sediments of this formation corresponds to deposition in evaporitic playa lakes (Alley & Lindsay 1998).

There is no evidence of marine transgression entering the Torrens basin from the South, which suggests an important subsidence of the Torrens basin since the Miocene when the sea-level was higher than today (Haq et al. 1987). At small length scale, subsidence in Lake Torrens is

assured by faults like the Ediacara fault (figure 24).

However, C  lerier et al. (2005) expect that the flexure mode might generate relief in the vicinity of Flinders Ranges, in response to any significant regional compression in the plate. This study explains the very low elevation of flanking basin like the Torrens basin by long-wavelength flexure resulting of stress field within the plate. Sandiford et al. (2004) have argued that the current tectonic regime is essentially a late Neogene phenomenon, reflecting changes in the Pacific-Australian plate coupling at around 10-6Ma. Long wavelength subsidence of Torrens basin is probably younger than Miocene.

During the sedimentation in Lake Billa Kalina, Torrens basin was probably at higher elevations and paleogeography can be in agreement with the hypothesis that a part of Torrens basin area was a part of the Billa Kalina Lake drainage area.

3.2.2 Lake Eyre

Lake Eyre consists of a thick sedimentary succession and much of the basin is close to sea level. Three paleogeographic phases are considered for the Eyre basin (Callen & Cowley 1995) :

1. Latest Paleocene to Middle Eocene with extensive fluvial environments (Eyre Formation).
2. Oligocene to Pliocene with extensive lake and associated fluvial and shoreline environments (Etadunna Formation).
3. Pliocene to Quaternary with fluvial, eolian and playa lake sediments.

The Eyre formation (Wopfner 1974) is a widespread and distinctive sand unit, lies unconformably on Mesozoic sediments and is overlain by the Miocene Etadunna Formation.

Datation of this formation (fossils and Carbonaceous horizons) gives an age of Late Paleocene to Middle Eocene.

Eyre Formation sediments are found in Poole Creek paleochannel (figure 12) and paleocurrents direction indicates a depocentre towards Lake Eyre (Ambrose & Flint 1980). Until at least the Oligocene-Early Miocene, water was transported from North-East of Billa Kalina basin to Lake Eyre basin. At the South West of Billa Kalina basin, paleocurrents are towards Eucla basin then the Billa Kalina basin was crossed by a drainage divide line during a part of the Eocene. The Etadunna Formation is a sequence dominated by white dolomitic carbonate with minor claystone and was deposited between late Oligocene and Late Miocene.

This formation is an essentially lacustrine and fluvial unit and streams had extensive floodplains (Callen & Plane 1985).

Currents directions in the lower Etadunna Formation channel facies of the Poole Creek paleochannel indicate deposition with a North to Northeasterly transport direction. There is no indication about paleocurrents in the upper Etadunna formation.

At the Oligocene - Early Miocene (lower Etadunna Formation) the Billa Kalina area was always a drainage divide, and this implies a relative higher topography. Because there is no current indication in the upper part of the Etadunna Formation, it is conceivable that inversion of topography occurred just before the filling of the Billa Kalina Lake (Early-Middle Miocene).

This inversion of topography can be the result of movements on faults like the Norwest fault (figure 16). In fact, motion on this fault is in agreement with uplift of Eyre basin relative to Billa Kalina basin. However, this is only an hypothesis and a more precise study of Lake Eyre basin is required to answer at this question.

3.2.3 Interpretations and conclusions

The study of adjacent areas gives us information about the evolution of the landscape during the Tertiary. Until at least the Early Miocene, the Billa Kalina basin was crossed by a drainage

divide between the Eucla basin and the Eyre basin. Then the Billa Kalina area was at higher elevations than the Eyre and Eucla basin until the Early Miocene. Paleochannels dated of the Early Oligocene - Early Miocene confirm that the depocentre was towards lake Eyre for the northern part of Billa Kalina basin at this time.

However, during the existence of Billa Kalina Lake (Early- Middle Miocene), the drainage area should contain a part of Torrens basin and Eyre basin areas. This implies that parts of Torrens basin and Eyre basins were at higher elevations than the paleolake. A first inversion of topography between Eyre basin and Billa Kalina basin occurred in the Early Miocene and it is possible to envisage the role of faults in this inversion. But we have not enough arguments to affirm this hypothesis.

From the deposition of the Willalinchina sandstone to recent times, the Billa Kalina basin is at higher elevations than Torrens basin and South part of Eyre basin. A relative subsidence should take place to explain present topography. C  lerier et al. (2005) suggests that young lithospheric flexure can explain low elevations of Torrens basin. But what phenomenon can explain the tilting of Lake Eyre area? In the following part, we propose a possible explanation.

3.3 Tomography and edge-driven convection

The topographic depression around Lake Eyre is a very large near circular low elevation region. An IDL program was written to represent the mean elevation of a circle area for given centre in function of the radius of the circle (figure 25). The centre of the topographic depression is around latitude $29^{\circ}4$ and longitude $137^{\circ}3$ and the radius varies from 0.1° to 5° .

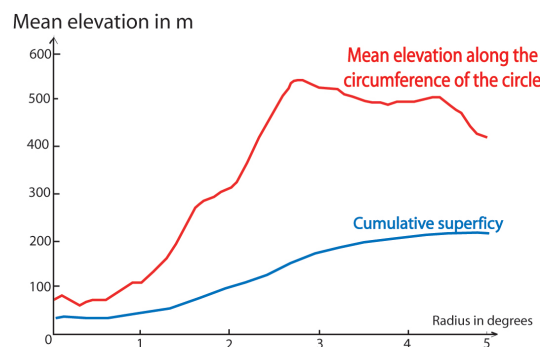


Figure 25: Cross-section through Tertiary sediments in the Torrens basin

The figure 25 shows that for radius superior as 4° , the mean elevation is constant. The depression is an approximate circle of 4° of radius. There are few large topographic depressions in the world but an example is the Hudson bay and several authors attribute this depression by convective downwelling within the mantle (James 1992, Peltier et al. 1992).

Several tomographies were done in Australia (Simons et al. 1999) and show lithospheric discontinuities within the plate (figure 26). Close to the lithospheric step, a downwelling in the mantle can be observed.

These lithospheric discontinuities can be responsible of edge-driven convection flow in the mantle as written in an article of King & Anderson (1998). A thermic model was carried out considering a lithospheric step and the result is that this discontinuity influences the mantle flow (figure 27). Close to the lithospheric step, a downwelling can be observed.

A downwelling flow in the mantle can be responsible of a near circular low topographic area as in the Hudson bay.

Edge-driven convection is a possible explanation of the subsidence in the Lake Eyre and Billa

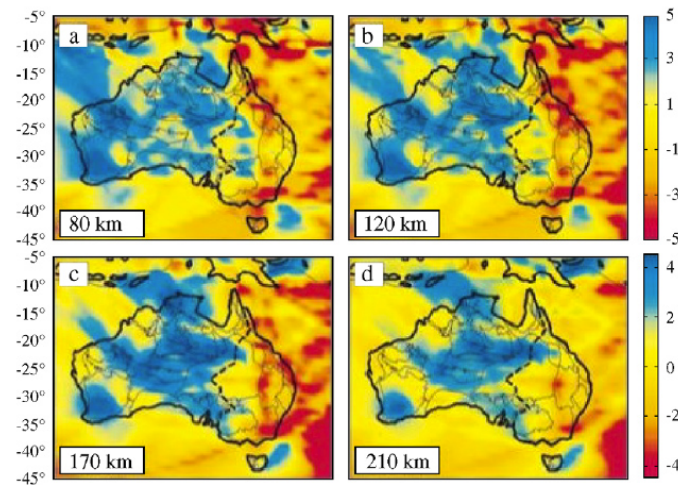


Figure 26: Depth slices through the preferred seismic velocity model the Australian continent and upper mantle. Anomalies are in percentage from a spherical reference model. Taken from Simons et al., 1999

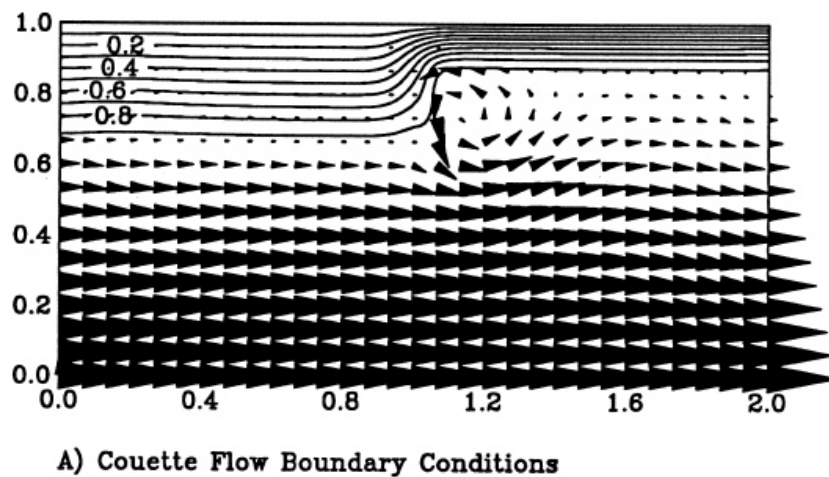


Figure 27: Flow field for edge-driven models with imposed Couette side-wall boundary conditions from King and Anderson, 1995.

Kalina area and it will be very interesting to build a numerical 3D-model which considers lithospheric structure in Lake Eyre area.

An interesting perspective would be to link Eyre and Eucla basin geological history. This would enable to have the landscape evolution of most part of the Australian continent.

Conclusion

The geomorphologic model I developed can be a useful tool to study geomorphology of an area. A simple example is presented in this report but the model will be used by an honours student of the University of Melbourne with a more data about all of the Whyalla's scarps. An interesting point of the modelling is the possibility of the quantification of different coefficient as well as the influence of fluvial processes in the shape of the landscape. An other perspective of this modelling can be to add the lithospheric flexure consequent of the sediment loading. Writing my own code makes easier future changes of the modelling and permits the addition of new functions.

Concerning the Eyre area, precise study of sedimentation in Lake Eyre basin can bring new observations of the tilting. An other point would be to develop a 3D numerical model of convective flux in the mantle considering Lake Eyre situation thanks to the tomography. In conclusion, this study can be seen like an introduction of different keys to study the landscape evolution and a lot of possibilities and improvements can be carried out.

References

- Alley, N. & Beecroft, A. (1993). Foraminiferal and palynological evidence from the pidinga formation and its bearing on eocene sea level events and palaeochannel activity, eastern eucla basin, south australia., *Mem. Assoc. Australasian Palaeontol.* **15**: 375–393.
- Alley, N. & Lindsay, J. (1998). *The Geology of South Australia - Chapter 10*, Vol. 2 : The Phanerozoic , Chapter 10 : The Tertiary, Mines and Energy - South Australia.
- Ambrose & Flint (1980). BILLA KALINA. south australia. explanatory notes. 1:250 000 geological series, *Geol. Surv. S. Aus.* pp. Sheet SH 53–7.
- Ambrose, G. & Flint, R. (1981). A regressive miocene lake system and silicified strandlines in northern south australia : implications for regional stratigraphy and silcrete genesis, *Journal of the Geological Society of Australia* **28**: 81–94.
- Andrews, D. & Hanks, T. (1985). Scarp degraded by linear diffusion : Inverse solution for age, *Journal of Geophysical Research* **90**: 10 193–10 208.
- Beaumont, C., Fullsack, P. & Hamilton, J. (1992). Erosional control of active compressional orogens, *Thrust Tectonics* pp. 1–18.
- Braun, J. & Sambridge, M. (1997). Modelling landscape evolution on geological time scales : a new method based on irregular spatial discretization, *Basin Research* **9**: 27–52.
- Buckman, R. & Anderson, R. (1979). Estimation of fault-scarp ages from a scarp-height-slope-angle relationship, *Geology* **7**: 11–14.
- Callen, R. (1981). FROME. south australia. explanatory notes and map sheet. 1:250 000 geological series, *South Australia Geol. Surv.* pp. Sheet SH/54–10.
- Callen, R. & Cowley, W. (1995). Billa kalina basin. in: Drexel, j.f., preiss, w.v. (eds.), the geology of south australia. volume 2. the phanerozoic., *South Aust. Dep. Mines Energy Bull.* pp. 195–198.
- Callen, R. & Plane, M. (1985). Stratigraphy drilling of cainozoic sediments near lake eyre, *BMR 1983 : Well completion report. Department of Mines and Energy.* pp. Report Book, 85/8.
- Chase, C. (1992). Fluvial landsculpting and the fractal dimension of the topography, *Geomorphology* **5**: 39–57.
- Christophel, D., Scriven, L. & Greenwood, D. (1992). The middle eocene megafossil flora of nelly creek (eyre formation), southern lake eyre, south australia., *Transactions of the Society of South Australia* **116**: 65–76.
- Célérier, J., Sandiford, M., Hansen, D. & Quigley, M. (2005). Modes of active intraplate deformation, flinders ranges, australia, *Tectonics* **24**: TC6006.
- Cowley, W. (1990). Early cambrian andamooka limestone and yarrowurta shale of the stuart shelf., *South Australia. Department of Mines and Energy. Report Book* **90/17**.
- Cowley, W. & Martin, A. (1991). KINGOONYA. south australia. explanatory notes. 1:250 000 geological series, *South Australia Geol. Surv.* pp. Sheet SH/53–11.

- Crone, A. J., Martini, P. M. D., Machette, M. N., Okumura, K. & Prescott, J. R. (2003). Paleoseismicity of two historically quiescent faults in Australia : Implications for fault behavior in stable continental regions, *Bulletin of Seismological Society of America* **93**(5): 1913–1934.
- ETSA (1989). *Stuart Creek, EL 1370. Lake Torrens, EL 1364. Lake Torrens West, EL 1397. Electricity trust of South Australia, Coal Resources Department*, **1**: 3–5.
- Greenwood, D., Callen, R. & Alley, N. (1981). The correlation and depositional environments of tertiary strata based on macroflora in the southern lake eyre basin, south Australia., *South Australia. Department of Mines and Energy. Report Book 90/15*: 81–94.
- Greenwood, D. R. (1996). Eocene monsoon forests in central Australia ?, *Australian Systematic Botany* **9**: 95–112.
- H. Kooi, C. B. (1994). Escarpment evolution on high-elevation rifted margins : insights derived from a surface processes model that combines diffusion, advection, and reaction, *Journal of Geophysical Research* **99**(B6): 12191–12209.
- Hanks, T., R.C. Buckman a, d. K. L. & Wallace, R. (1984). Modification of wave-cut and faulting-controlled landforms, *Journal of Geophysical Research* **89**: 5771–5790.
- Haq, B. U., Hardenbol, J. & Vail, P. R. (1987). Chronology of fluctuating sea levels since the triassic, *Science* **235**: 1156–1167.
- Howard, A., Dietrich, W. & Seidl, M. (1994). Modeling fluvial erosion on regional continental scales, *Journal of Geophysical Research* **99**: 13971–13986.
- Jack, R. (1914). Geol. surv. south Australia, *Bulletin* **3**.
- James, T. (1992). The hudson bay free-air gravity anomaly and glacial rebound, *Geophysical Research Letters* **19**(9): 861–864.
- Johns, R., Hiern, M. & Nixon, L. (1966). ANDAMOOKA. south Australia. explanatory notes. 1:250 000 geological series.
- King, S. D. & Anderson, D. L. (1998). Edge driven convection, *Earth and Planetary Science Letters* **160**: 289–296.
- Krieg, G., Rogers, P., Callen, R., Freeman, P., Alley, N. & Forbes, B. (1991). CURDIMURKA. south Australia. explanatory notes. 1:250 000 geological series, *South Australia Dep. Mines Energy* .
- Lague, D. (2001). *Dynamique de l'érosion continentale aux grandes échelles de temps et d'espace : Modélisation expérimentale, numérique et théorique*, PhD thesis, Université de Rennes.
- Miles, K. R. (1951). Tertiary faulting in north-eastern eyre peninsula, south Australia, *Trans. Roy. Soc. S. Aust., Department of Mines, South Australia* pp. 89–96.
- Peltier, W., Forte, A., Mitrovica, J. & Dziewonski, A. (1992). Earth's gravitational field : seismic tomography resolves the enigma of Laurentian anomaly, *Geophysical Research Letters* **19**(15): 1555–1558.
- Pitt, G. (1978). Murloocoppie , south Australia, *South Australia. Geological Atlas 1:250 000 Series - Explanatory Notes* pp. Sheet SH53–2.

- Sandiford, M. (2003). Neotectonics of southeastern australia : Linking the quaternary faulting record with seismicity and in situ stress, *Evolution and Dynamics of the Australian Plate*, edited by R.R. Hillis and D. Muller, *Spec. Publ. Geol. Soc. Aus.* **22**: 101–113.
- Sandiford, M., Wallace, N. & Coblenz, D. (2004). Origin of the in situ stress field in southeastern australia, *Basin Research* **16**: 325–338.
- Selby, M. (1993). Hillslope materials and processes, *Oxford University Press* p. 450pp.
- Simons, F., Zielhuis, A. & van der Hilst, R. (1999). The deep structure of the australian continent from surface wave tomography, *Lithos* **48**: 17–43.
- Tucker, G. & Whipple, K. (2002). Topographic outcomes predicted by stream erosion models : Sensitivity analysis and intermodel comparison, *Journal of Geophysical Research* **107**(B9): 2179.
- Wallace, R. (1977). Profiles and ages of young fault scarps, north-central nevada, *Geol. Soc. Am. Bull.* **88**: 1267–1281.
- Wopfner, H. (1974). Post-eocene history and stratigraphy of north-eastern south australia. royal society of south australia., *Transactions* **98**: 1–12.
- Zang, W.-L., Alley, N., Rowett, R. & Broadbridge, L. (2006). Tertiary willalinchina and watchie sandstones and fossil floras. billa kalina basin, south australia, *Article in preparation* .

APPENDIX

A Code

```

PRO faille__define
;Define the structure of the class : faille
;All of this variables will be used in the following methods
;DECLARATION :
struct={faille,          $;Name of the structure
level_noise:0,          $;Noise on the surface
dim:0,                  $;Dimension of the square grid (number of nodes along a side)
dist:0,                 $;distance between each node
rain:PTR_NEW(/allocate),          $;quantity of precipitation above the grid
ground2:PTR_NEW(/allocate),       $;topography of the ground
ground3:PTR_NEW(/allocate),       $;topography of the ground initial (for memory)
transmit:PTR_NEW(/allocate),$;Coordonates of the receiver node (water flow)
diffu:PTR_NEW(/allocate),         $;Diffusivity coefficient (for each node)
delta_t:0                ,      $;Time step
rate:0.000               ,      $;Elevation rate
kf:PTR_NEW(/allocate),   $;Long range transport coefficient (for initial rock)
resis_sed:0 ,           $;Long range transport coefficient for the alluvial sediments
number_loop:0 ,        $;Number of loop
slope:PTR_NEW(/allocate),$;Value of the gradient with the neighbours of a node
sedi:PTR_NEW(/allocate) ,   $;Amount of sediment in each node
somme:PTR_NEW(/allocate) ,  $;Variable used for the inversion
model:PTR_NEW(/allocate),   $;Variable used for inversion
z4:fltarr(195),            $;Variable which contains the GPS data (from field work)
num:0,                    $;Number of the loop during the running
tri:PTR_NEW(/allocate)}    ;Sort of the elevation variable (ground2)
END

;-----

FUNCTION faille::init ;INITIALISATION : first value of each variable

;DO NOT CHANGE :-----
self.diffu=PTR_NEW(fltarr(self.dim,self.dim)) ;SHORT RANGE coefficient
self.ground2=PTR_NEW(fltarr(self.dim,self.dim))
self.ground3=PTR_NEW(fltarr(self.dim,self.dim))
self.tri=PTR_NEW(fltarr(self.dim,self.dim))
self.sedi=PTR_NEW(fltarr(self.dim,self.dim))
self.model=PTR_NEW(fltarr(self.number_loop+2,195))
self.rain=PTR_NEW(fltarr(self.dim,self.dim))
self.transmit=PTR_NEW(fltarr((self.dim)*(self.dim),2))
self.slope=PTR_NEW(fltarr(((self.dim)*(self.dim)),8))
self.kf=PTR_NEW(fltarr(self.dim,self.dim)) ;for the Long range
self.num=0 ; self.z4=fltarr(195)
self.somme=PTR_NEW(fltarr(self.number_loop+1))
;-----

```

```

;CHANGE THIS :
-----
self.number_loop=7200 ;Number of loop

self.dim=50          ;Length of the side of the area (eq number of
nodes)
self.dist=14        ;Distance between each node in m ;
self.level_noise=1  ;Level of noise (instability) ;
  for m=0,(self.dim*self.dim)-1 do begin ;

(*self.diffu)[m]=0.0005 ;Value of the diffusivity coefficient

endfor

self.delta_t=62.5 ; Time step : a loop <=> self.delta_t years;
self.rate=(42./(1+ self.number_loop/100)) ;Uplift in m (here=42m)
;Definition of kf (long-range coefficient) in function of the
;localisation on the grid
  for i=round(self.dim/2),self.dim-1 do begin
    for j=round(self.dim/2),self.dim-1 do begin
      (*self.kf)[i,j]=1e-4
    endfor
  endfor
endfor
  for i=0,round(self.dim/2) do begin
    for j=round(self.dim/2),self.dim-1 do begin
      (*self.kf)[i,j]=1e-4
    endfor
  endfor
  for i=0,(self.dim-1) do begin
    for j=0,round(self.dim/2)+1 do begin
      (*self.kf)[i,j]=1e-4
    endfor
  endfor
self.resis_sed=8e-4 ;resistance of the alluvial sediments return,1
END
;-----
PRO faille::geo2 ;It's the main program
;Initial ground :
self -> create_ground
self->create_z4 ;Read the GPS data from the field work
self->fault1 ; Initial mouvement on the fault
;;Loops :
  for i=0,self.number_loop do begin
    self.num=i
    if ( (i mod (50000/self.delta_t)) eq 0 ) then begin
      print,'uplift here ..... '
      self->fault ;Uplift corresponding of the fault
    endif
    self->MAKE_RAIN ; Make the precipitations
  endfor

```

```

    self -> MAKE_FLOW ;Flow of water above the ground
    self->RESIS ; define the variation of resistance (if alluvial sediments)
    self->SHORT_RANGE ; Short-range erosion
    self->LONG_RANGE
    self->inversion ; Compare GPS data and modelling results
;GRAPHIC REPRESENTATION :
if ((i mod 100) eq 0) then begin
    self->plot_ground
    self->view
    window,1
    self->plot_profiriver
    tab=TVRD()
    WRITE_BMP,int2ext2(self.num) + "profiriver.bmp",tab
;Un-comment this for writing .bmp at each time step :
    self -> PLOT_ground
    tab=TVRD()
    WRITE_BMP, int2ext2(self.num) + ".bmp",tab
    self -> plot_profil
    tab=TVRD()
    WRITE_BMP,int2ext2(self.num) + "profi.bmp",tab
;Export elevation grid in a txt file :
    self->output
endif
endfor

;Find the better agreement between modelling and data :
mieux=where(min(*self.somme) eq *self.somme)
print,mieux
plot,(*self.model)[mieux,*]
oplot,(*self.model)[self.number_loop+1,*]
END
;-----
;Function for creating the ground
PRO faille :: create_ground
    for i= 0,(self.dim*self.dim)-1 do begin
        (*self.ground2)[i]=48 + (self.level_noise*abs(randomn(s,1)))
    endfor
    for i=0,self.dim-1 do begin
        for j=0,ceil(self.dim/2) do begin
            variable=float((self.dim/2)-j)
            variable=(variable/ceil(self.dim/2))
            (*self.ground2)[i,j]+=variable * 10 ;slow dipping for drainage area
        endfor
    endfor
END
;-----
;Function for creating the fault 0141 PRO faille :: fault
for i=0,round(((self.dim*self.dim)-1)*0.42) do begin
    (*self.ground2)[i]+=self.rate
    (*self.ground3)[i]+=self.rate

```

```

endfor
END
;-----
;Initial motion along the fault
PRO faille :: fault1
  for i= 0,round(((self.dim*self.dim)-1)*0.42) do begin
    (*self.ground2)[i]+=0.4
    (*self.ground3)[i]+=0.4
  endfor
END
;-----
PRO faille :: PLOT_GROUND ; Plot the surface
;View of the surface :
loadct,9
DEVICE, DECOMPOSED = 0
WINDOW, 0, XSIZE=600, YSIZE=350,TITLE = 'Surface '
shade_surf,*self.ground2,AZ=190,AX=50, ZSTYLE=4,YSTYLE=4,XSTYLE=4; ,ZRANGE =[1000,2000]
END
;-----
PRO faille::plot_profi1 ; Plot a diffusive profile
profi=fltarr(self.dim)
  for i=0,self.dim-1 do begin
    profi(i)=(*self.ground2)[1,i]
  endfor
  profi=congrid(profi,195)
  plot,profi; ,YRANGE = [0,1150]
  oplot,(*self.model)[self.number_loop+1,*]
END
;-----
PRO faille::plot_profi2 ; Plot a second diffusive profile
profi=fltarr(self.dim)
  for i=0,self.dim-1 do begin
    profi(i)=(*self.ground2)[round(self.dim/2),i]
  endfor
plot,profi,YRANGE = [900,1150] END
;-----
PRO faille::plot_profiriver ; Plot a profile along a river
compteur=0
profi=fltarr(200) ;Find the first point of a river
  for m=0,n_elements(*self.tri)-1 do begin
    x=where(max(*self.rain) eq *self.rain )
    profi(0)=(*self.ground2)[x]
    while ((*self.rain)[x] gt self.delta_t ) do begin
      d1=fltarr(8)
      d2=fltarr(8)
      t=0
      for i=0,n_elements(*self.ground2)-1 do begin
        if (x eq (*self.transmit)[i,0]) then begin
          print,t
          d1(t)=i
        end
      end
    end
  end

```

```

                d2(t)=(*self.rain)[i]
                t=t+1
            endif
        endfor
        for j=0,n_elements(d1)-1 do begin
            if (d1(j) eq x) then begin
                d2(j)=0
            endif
        endfor
        indice=where(d2 eq max(d2))
        profi(compteur)=(*self.ground2)[(*self.transmit)[d1(indice),0]]
        x=d1(indice)
        if (n_elements(x) gt 1) then begin
            x=x(1)
        endif
        compteur=compteur+1
    endwhile
endfor
f=0
for t=0,n_elements(profi)-1 do begin
    if (profi(t) ne 0) then begin
        f+=1
    endif
endfor
newprofi=fltarr(f)
for t=0,f-1 do begin
    newprofi(t)=profi(t)
endfor
newprofi=reverse(newprofi)
window,1
plot,newprofi,YRANGE = [min(newprofi)-10,max(newprofi)+10]
END

```

```

;-----

```

```

PRO faille::MAKE_RAIN ;Create the precipitation array
;Rain : Randomn function
for k=0,(self.dim*self.dim)-1 do begin
    (*self.rain)[k]=1*self.delta_t
endfor
END

```

```

;-----

```

```

PRO faille::MAKE_FLOW

```

```

-----

```

```

; Each node has a maximum of 8 neighbours. In all this procedure,
neighbours have got the following numbers :

```

```

|   0   |   1   |   2   | ;
|   7   | NODE k |   3   | ;
|   6   |   5   |   4   | ;

```

```

; For a node which has 8 neighbours (not border's node) the

```

variable f takes : ; f(k,*) = [0,1,2,3,4,5,6,7]
 ; For the borders and edge, a node haven't got 8 neighbours.

For example, for the first node (Top left of the grid) neighbours n°
 0,1,2,6 and 7 don't exist. When a neighbour don't exist, the
 corresponding value of f takes 9. For this example, we have :

f(0,*) = [9,9,9,3,4,5,9,9]

```

-----
f=intarr((self.dim*self.dim),8) ;Initialisation
for k=0,((self.dim)^2)-1 do begin ; for all the grid
  f(k,*)=[0,1,2,3,4,5,6,7]
endfor
for k=1,(self.dim-2) do begin ;Top Border
  f(k,*)=[9,9,9,3,4,5,6,7]
endfor
for k=((self.dim)*(self.dim-1)+1),((self.dim)^2)-2 do begin
;Bottom border
  f(k,*)=[0,1,2,3,9,9,9,7]
endfor
for k=self.dim,(self.dim*(self.dim-2)),self.dim do begin
; Left Border
  f(k,*)=[9,1,2,3,4,5,9,9]
endfor
for k=(2*self.dim)-1,(self.dim*(self.dim-1)-1),self.dim do begin
;Right Border
  f(k,*)=[0,1,9,9,9,5,6,7]
endfor
f(0,*)=[9,9,9,3,4,5,9,9] ; Top Left Corner
f((self.dim)-1,*)=[9,9,9,9,9,5,6,7] ;Top Right Corner
f((self.dim)*(self.dim-1),*)=[9,1,2,3,9,9,9,9];Bottom Left Corner
f(((self.dim)^2)-1,*)=[0,1,9,9,9,9,9,7] ; Bottom Right Corner
;Distance is a 8 value variable and it is the distance between the
;considerating node and its neighbour, [function of the neighbour
(same order as before)]
distance=[(self.dist*sqrt(2)),self.dist,(self.dist*sqrt(2)),self.dist,$
(self.dist*sqrt(2)),self.dist,(self.dist*sqrt(2)),self.dist]
;p is a value variable which contains the number of the neighbour, it is a
k function
for k=0,((self.dim)^2)-1 do begin
  p=[k-(self.dim)-1,k-(self.dim),k-(self.dim)+1,k+1,$
  k+(self.dim)+1,k+(self.dim),k+(self.dim)-1,k-1]
  for i=0,7 do begin
    if (f(k,i) ne 9) then begin ; If there is a neighbour (f non equal 9)
      ;Slope = difference of elevation / distance between two nodes :
      (*self.slope)[k,i]=((*self.ground2)[p(i)]-(*self.ground2)[k])/distance(i)
    endif
  endfor
endfor
;From the highest to the lowest point, find the most important

```

negative slope

;and deplace the water from the considering node
to its lowest neighbour

;The variable transmit remember the
coordonates of the lowest neighbour

;and the associating slope for
each node of the grid

```
*self.tri=reverse(sort(*self.ground2))
  for m=0,n_elements(*self.tri)-1 do begin
    k>(*self.tri)[m]
    p=[k-(self.dim)-1,k-(self.dim),k-(self.dim)+1,k+1,  $
      k+(self.dim)+1,k+(self.dim),k+(self.dim)-1,k-1] ;
    minimum=min((*self.slope)[k,*])
    if (minimum lt 0) then begin
      for i=0,7 do begin
        if (f(k,i) ne 9) then begin
          if ((*self.slope)[k,i] eq minimum )then begin
            (*self.transmit)[k,0]=p(i) ; number of the node
            (*self.transmit)[k,1]=((*self.slope)[k,i]; value of the slope
            (*self.rain)[(*self.transmit)[k,0]]+=(*self.rain)[k]
          endif
        endif
      endfor
    endif else begin
      (*self.transmit)[k,0]=k
    endif
  endfor
```

END

;-----

PRO faille::SHORT_RANGE

;Calcul the short range erosion

;A simple diffusion equation is used :

for k=0,((self.dim)^2)-1 do begin

for i=0,7 do begin

(*self.ground2)[k]+=(((*self.diffu)[k]*(*self.slope)[k,i]*self.delta_t))

endfor

endfor

END

;-----

PRO faille::LONG_RANGE ; Second long range (different in
programming formulation)

fluvial=fltarr(self.dim*self.dim)

erosion=fltarr(self.dim,self.dim)

sediment=fltarr(self.dim,self.dim)

for m=0,(n_elements(*self.tri)-1) do begin

k>(*self.tri)[m]

fluvial(k)=abs(((self.kf)[m])*(((self.rain)[k])^(1.3))* \$
 (((self.transmit)[k,1])))*(0.2)

erosion(k)+= (-fluvial(k))

```

        sediment((*self.transmit)[k,0])+= fluvial(k)
    endfor
*self.sedi+=erosion+sediment
*self.ground2+=erosion+sediment
;isurface,*self.sedi
END
;-----
PRO faille::RESIS
for m=0,round((n_elements(*self.tri)-1)/2) do begin
    if ((*self.sedi)[m] gt 0) then begin
        (*self.kf)[m]=self.resis_sed
    endif
endif
endfor
for m=round(((self.dim*self.dim)-1)/2)+self.dim,(n_elements(*self.ground2)-1) do begin
    if ((*self.ground2)[m] gt (*self.ground3)[m]) then begin
        (*self.diffu)[m]=0.002
    endif
endif
endfor
END
;-----
PRO faille::output ; Export elevation data in a txt file
temp=string(reverse(*self.ground2))
openw,1, int2ext2(self.num)
WRITEU, 1, temp
; Close file unit 1:
CLOSE, 1
END
;-----
PRO faille::view;
Use object-programming to represent the surface
COMMON COLORS, r_orig, g_orig, b_orig, r_curr, g_curr,b_curr
max_data = max(*self.ground2) 0368 min_data = min(*self.ground2)
;Creating an image (jpg : RGB then 3 dimensions)
image = (BYTARR(3,self.dim, self.dim))
;definition d'une table de couleurs
r_curr = interpol([0,33,64,141,205,205], 256)
g_curr = interpol([90,134,135,158,196,200], 256)
b_curr = interpol([6,2,2,2,56,117], 256)
image(0,*,*)=r_curr[hist_equal(*self.ground2 , MINV = min_data, MAXV = max_data)];
image(1,*,*)=g_curr[hist_equal(*self.ground2, MINV = min_data, MAXV = max_data)];
image(2,*,*)=b_curr[hist_equal(*self.ground2 , MINV = min_data,MAXV = max_data)];
imageSize = [self.dim,self.dim]
;oWindow = OBJ_NEW('IDLgrWindow', RETAIN = 2,COLOR_MODEL=0 $
, TITLE = 'first step in Graphics Object Programming !')
oView = OBJ_NEW('IDLgrView')
oModel = OBJ_NEW('IDLgrModel')
oSurface=OBJ_NEW('IDLgrSurface',*self.ground2,STYLE=2)
oImage = OBJ_NEW('IDLgrImage', image , interleave=0 , /INTERPOLATE)
oSurface -> GETPROPERTY, X RANGE=xr , Y RANGE=yr , Z RANGE=zr
xs=NORM_COORD(xr)

```

```

xs[0]=xs[0]-0.5
ys=NORM_COORD(yr)
ys[0]=ys[0]-0.5
zs=NORM_COORD(zr)
zs[0]=zs[0]-0.5
oSurface->SETPROPERTY , XCOORD_CONV = xs , YCOORD_CONV=ys,ZCOORD_CONV=zs
oSurface -> SetProperty , TEXTURE_MAP = oImage , color=[255,255,255]

; add directional light
mylight = OBJ_NEW('IDLgrLight',TYPE=2,LOCATION=[15,30,30],color=[255,255,255])
mylight->SetProperty, INTENSITY=5
oModel->Add, mylight

;add ambient light 0403
mylight_amb = OBJ_NEW('IDLgrLight',TYPE=0,LOCATION=[15,15,50],color=[255,155,155])
mylight_amb->SetProperty,INTENSITY=0.1
oModel->Add, mylight_amb
;Add my light to my model
oModel -> Add, oSurface
sx = 1 & sy = 1 & sz = 0.2
oModel->Scale,sx, sy, sz
oView -> Add, oModel
oModel -> ROTATE, [1,0,0], 80
oModel -> ROTATE, [0,1,0], -35
oModel -> ROTATE, [0,0,1], 185
oWindow -> Draw, oView
oClipboard = OBJ_NEW('IDLgrClipboard', QUALITY = 2, $
    DIMENSIONS = windowSize, $
    RESOLUTION = screenResolution,$
    GRAPHICS_TREE = oView)
oClipboard->Draw, FILENAME = int2ext2(self.num)+'file.eps', $
    /POSTSCRIPT, /VECTOR
oClipboard->SetProperty, GRAPHICS_TREE = OBJ_NEW()
OBJ_DESTROY, oClipboard
OBJ_DESTROY, oWindow
xobjview,oModel ;, stat=[mylight,mylight_amb]
END
;-----
PRO faille::create_z4 ; Read the GPS data
data = READ_ASCII('test4.txt', DATA_START=0 , NUM_RECORDS=490)
x=intarr(n_elements(data.field1)/2)
z=fltarr(n_elements(data.field1)/2)
j=0
for i=0,(n_elements(data.field1))-1,2 do begin
    x(j)=data.field1(i)
    z(j)=data.field1(i+1)
    j=j+1
endfor
x2=intarr(n_elements(data.field1)/2)
z2=fltarr(n_elements(data.field1)/2)

```

```

classement=sort(x)
for i=0,(n_elements(x)-1) do begin
    x2(i)=x(classement(i))
    z2(i)=z(classement(i))
endfor
x3=findgen(max(x2))
z3=interpol(z2,x2,x3)
x3=congrid(x3,200)
z3=congrid(z3,200)
;Mean
for i=0,n_elements(x3)-6 do begin
    self.z4(i)=(z3(i)+z3(i+1)+z3(i+2)+z3(i+3)+z3(i+4)+z3(i+5))/6
endfor
x4=findgen(n_elements(self.z4))
(*self.model)[self.number_loop+1,*]=self.z4
END
;-----
PRO faille::inversion
;;;:~::~~::~~::~~::~~::~~::~~::~~::~~::~~::~~::~~::~~::~~::~~::~~::~~::~~::~;
;-----;
;;;:~::~~::~~::~~::~~::~~::~:Inversion Method ~::~~::~~::~~::~~::~~::~;
;-----;
;;;:~::~~::~~::~~::~~::~~::~~::~~::~~::~~::~~::~~::~~::~~::~~::~~::~~::~~::~;
temp=fltarr(self.dim)
temp(*)=(*self.ground2)[1,*]
temp=congrid(temp,195)
(*self.model)[self.num,*]=temp(*)
diff=abs(((self.model)[self.num,*]* $
    (*self.model)[self.num,*])-(self.z4*self.z4))
(*self.somme)[self.num]=total(diff)
;print,self.num
END

```